



Cite this: *Nanoscale*, 2022, **14**, 3987

## Advanced metal and carbon nanostructures for medical, drug delivery and bio-imaging applications

Neeraj Kumar,<sup>a,b</sup> Pankaj Chamoli, <sup>c</sup> Mrinmoy Misra, <sup>d</sup> M. K. Manoj<sup>b</sup> and Ashutosh Sharma <sup>\*e</sup>

Nanoparticles (NPs) offer great promise for biomedical, environmental, and clinical applications due to their several unique properties as compared to their bulk counterparts. In this review article, we overview various types of metal NPs and magnetic nanoparticles (MNPs) in monolithic form as well as embedded into polymer matrices for specific drug delivery and bio-imaging fields. The second part of this review covers important carbon nanostructures that have gained tremendous attention recently in such medical applications due to their ease of fabrication, excellent biocompatibility, and biodegradability at both cellular and molecular levels for phototherapy, radio-therapeutics, gene-delivery, and biotherapeutics. Furthermore, various applications and challenges involved in the use of NPs as biomaterials are also discussed following the future perspectives of the use of NPs in biomedicine. This review aims to contribute to the applications of different NPs in medicine and healthcare that may open up new avenues to encourage wider research opportunities across various disciplines.

Received 19th November 2021,  
Accepted 15th January 2022

DOI: 10.1039/d1nr07643d

rsc.li/nanoscale

### 1. A brief history of nanostructures

Nanomaterials are materials with a dimension range less than or equal to  $10^2$  nanometers. A nanoparticle (NP) is one-millionth of a millimeter in diameter or  $10^5$  times smaller than the diameter of a human hair. Physics, chemistry, and engineering researchers are prompted to research nanotechnology to develop future nanoproducts as a result of interesting phenomena happening at the nanoscale.<sup>1</sup> What is the use of nanoparticles? What sets “nano” apart? The term “nano” refers to something that is extraordinarily tiny. When a material’s dimension is shrunk from a large size, its qualities initially remain the same, but minor changes occur until the size is lowered to  $10^2$  nm where significant changes in properties occur. These dimensions have high surface-to-volume ratios linked to the quantum size effects.<sup>2</sup> As the particle gets smaller, a higher fraction of atoms accumulates on the surface and grain boundaries. This raises the surface-to-volume ratio,

resulting in more atoms on the surface than in the crystalline lattice.<sup>3</sup> Quantum physics, rather than classical mechanics, governs the physical characteristics due to their minuscule size. As the continuum transitions between the electrical bands become distinct, the characteristics of nanomaterials become reliant on their size. Aside from that, particle characteristics like electrical conductivity and optical property, color, and strength change greatly from their macro counterparts due to particle size and shape.<sup>4–6</sup>

The variety of uses for nanomaterials increases as particle size decreases to the nanoscale range.<sup>6</sup> In this respect, NPs of noble metals and semiconductors have outstanding properties and applications. While bulk silver (Ag) is non-toxic, silver nanoparticles (AgNPs) seem to be likely to kill harmful bacteria upon contact. In addition, nanomaterials may be built atom by atom utilizing bottom-up or top-down approaches. Material building blocks include embedded information, which is used throughout the production process to construct the final product. As a result of their various characteristics, NPs can also have combined properties that are different from those of nanoparticles and bulk samples with the same material. They might be employed in a variety of industries, including nanoelectronics, sensors, and single-electron transistors. Nanoscale materials may have their optical, mechanical, electrical, magnetic, and chemical characteristics altered by small changes in size, shape, and composition.<sup>7</sup>

Nowadays, nanomaterials are the main topic of conversation because of their potential to solve certain fundamental quantum size effect concerns by restricting the number of free electrons,

<sup>a</sup>Department of Metallurgical Engineering, SOE, O.P. Jindal University, Raigarh 496109, India

<sup>b</sup>Department of Metallurgical and Materials Engineering, NIT Raipur, Raipur, 492010, India

<sup>c</sup>School of Basic & Applied Sciences, Department of Physics, Shri Guru Ram Rai University, Dehradun-248001, Uttarakhand, India

<sup>d</sup>Department of Mechatronics, School of Automobile, Mechanical and Mechatronics, Manipal University Jaipur, 303007 Rajasthan, India

<sup>e</sup>Department of Materials Science and Engineering, Ajou University, Suwon-16499, South Korea. E-mail: stannum.ashu@gmail.com; Fax: +82-31-219-1613; Tel: +82-10-95345040

as well as their potential use as sophisticated materials. NPs have been widely used in a wide range of fields, such as cosmetic products and medicines, storage systems, fuel cells, semi-conductors, catalysis, and sensor systems. Rather than treating the entire body, only the influenced cells and tissues are treated.<sup>8–10</sup> Nanomaterials allow the identification of defined targets, such as specific cells or tissues, and the selection of suitable nano-carriers to yield the desired performance while reducing adverse effects.<sup>11,12</sup> Recent attention has been drawn to studies of metal NPs, especially noble metal NPs because of their unique characteristics among all nanoparticles. The fabrication of nanomaterials will be covered in the following paragraphs.

## 2. Synthesis methods of nanoparticles

The most important and groundbreaking field in nanoscience is the vast variety of nanomaterials. The formulation of NPs can be achieved in two ways: (1) top-down and (2) bottom-up methods, as highlighted in Fig. 1.

The dimension of the bulk crystal reduces down to the range of nanometers in the top-down phase by applying

different chemical and physical approaches. External variables, *e.g.*, friction and pressure, constrain the particles in the desired shape and sizes to reduce in dimension.<sup>13,14</sup> In recent times, for instance, many initiatives, such as ball milling, have been used in the handling of nanoscale materials,<sup>15</sup> including the lithography process,<sup>16</sup> pyrolysis process,<sup>17</sup> and the thermolysis process.<sup>18</sup> However, the top-down techniques have some drawbacks, *e.g.*, large size variation, residual stresses, and therefore more surface defects. In addition, this process is less cost-effective because of the high-pressure environment, elevated temperatures, and extremely advanced nanostructured material processing equipment.

Ball milling consists of milling the microparticles down to NPs by using high-energy ball milling equipment. During the milling process, the collision amongst the balls and vials of the mill under a certain rotating speed (revolutions per minute, rpm) causes the breakdown of the microparticles to NPs. Additionally, certain process parameters such as milling atmosphere, process control media, rpm, ball-to-powder mass ratio, milling duration, and temperature must be further optimized to achieve a definite size of NPs.<sup>19,20</sup>

Lithography is also a popular top-down method to synthesize NPs and complex 2D and 3D nanoscale patterns with



Neeraj Kumar

Prof. Neeraj Kumar is Senior Assistant Professor in the Department of Metallurgical Engineering, SOE, OP Jindal University, Raigarh, Chhattisgarh, India. He obtained an M.Tech in Metallurgical Engineering from Thapar University, Patiala, Punjab and holds a Masters degree from Chaudhary Charan Singh University (formerly, Meerut University), Uttar Pradesh, and Ph.D. in Metallurgical Engineering from NIT Raipur, Chhattisgarh, India. Prof. Neeraj has 12 years' plus experience teaching at the engineering graduate and postgraduate levels. Additionally, he works on different research areas of nanotechnology, including electrochemical corrosion, composites, nanostructured materials, wear, aluminium and its composites, and also on various automotive engineering applications. Prof. Neeraj has already been granted 3 international patents (Australia, Germany) and one more German patent has been filed. He has published 15+ research papers in international journals of repute, written 2+ book chapters, and presented 12+ papers at national and international conferences in various countries like the UAE, Nepal, and South Korea.



Pankaj Chamoli

Dr Pankaj Chamoli is an Associate Professor, Department of Physics, Sri Guru Ram Rai University, Dehradun, Uttarakhand, India. He received his Ph.D. in Materials Science from the Materials Science Programme, IIT Kanpur, Kanpur, Uttarpradesh, India. He obtained an M.Tech. in Materials & Metallurgical Engineering from Thapar University, Patiala, Punjab, and holds graduate and post-graduate (Physics) degrees from HNB Garhwal University, Srinagar, Uttarakhand. Dr Chamoli has 5 years experience in teaching to undergraduate level and higher levels. Additionally, he is an active researcher, and enthusiastically participates in cutting-edge research and innovation. He is working on different areas of nanoscience and technology, particularly focusing on nano-structured materials, carbon nano-materials (Graphene), nano-composites, nano-colloids, soft materials and their utilization for water purification, photocatalytic activity, microwave absorption, energy storage/conversion, and various biological applications. Dr Chamoli has filed 3 Indian patents, and one Indian patent has been granted in 2020. He has published 3+ book chapters, 22+ research papers in international journals of repute, and presented 20+ papers at National/International conferences. Dr Chamoli is an active reviewer for various high impact journals of Elsevier & Springer.

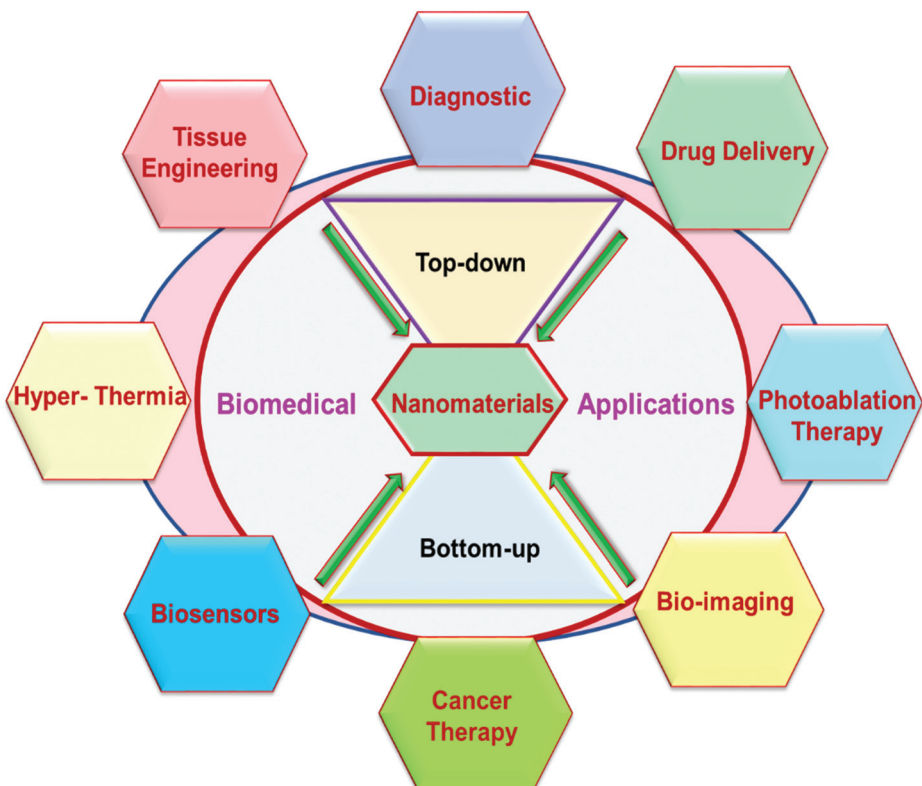


Fig. 1 Synthesis methods of various NPs and their various biomedical applications.



Mrinmoy Misra

Dr Mrinmoy Misra is an Assistant Professor in the Department of Mechatronics Engineering, Manipal University Jaipur, India. He received his Ph.D. from the Academy of Scientific and Innovative Research (AcSIR), in September 2015. After being a postdoctoral researcher in the Indian Institute of Technology Kanpur, India (April 2015–March 2016) and the Research Institute of Battery and Energy Conservation, Gachon University, South Korea (Sep. 2016 to March 2018) and an Assistant Professor at Gachon University, South Korea (April 2018 to March 2020), he joined as an Assistant Professor at Manipal University Jaipur, India. His main research areas are transparent conducting thin film heater fabrication and nanomaterial-based energy generation and core-shell nanomaterial synthesis and application.



M. K. Manoj

Dr Manoranjan Kumar Manoj is an Assistant Professor and Head of the Department of Metallurgical and Materials Engineering at NIT Raipur, Chhattisgarh, India. Dr Manoranjan received his Ph.D. in Metallurgical Engineering from IIT Roorkee, an M.Tech in Metallurgical Engineering from IIT Roorkee, and a B.Sc in Metallurgical Engineering from BIT Sindri, India. Dr Manoranjan has 16+ years of experience teaching at the engineering graduate and postgraduate levels. Further, Dr Manoranjan is working on research areas of thermodynamics, nanotechnology, corrosion, structure–property correlation, tribology, and welding. He has published 25+ research papers in international journals of repute, written 3+ books, and presented 15+ papers at national and international conferences. Dr Manoranjan has served as the convener of 10+ national and international conferences and workshops. During his academic duties, Dr Manoranjan also supervised the Ph.Ds of 4+ students. He has also been granted 2+ international patents and some are in the process of filing. Dr Manoranjan serves as a reviewer and editorial board member for over 10 prestigious journals.

better control of the structure. By introducing photolithography, soft-lithography, imprint lithography, and scanning probe-lithography (SPL) to a substrate surface, the desired pattern can be electronically synthesised and processing can be used. In the field of electronic circuit synthesis and processing of electronics components,<sup>21–25</sup> this approach can be used.

Pyrolysis is a further top-down technique for processing NPs on a large scale. Organic matter is disintegrated using this technique at a recognized maximum temperature as the pyrolytic temperature in the absence of an oxidizing agent, generally 300 °C–900 °C. A high-temperature and high-pressure annealing of the resulting decomposed mass produces well-defined NPs. The obtained NPs are often aggregates with a large distribution of particle sizes. This method may not be inexpensive since it takes great pressure and temperature, but it is also used for processing on a commercial scale.<sup>26</sup>

In the bottom-up methods, an array of atoms is created and stacked layer by layer until the desired structure is obtained. These atoms, however, originate from their respective ions and salts by reduction with appropriate chemical reagents.<sup>27</sup> Bottom-up nanostructures have lower surface defects and good atomic packaging to minimize the total Gibbs free energy and provide greater reliability compared to the top-down method, and further expand the applications of NPs. There is a variety of familiar approaches from bottom to top. For example, in chemical synthesis, an effective reduction agent is typically used for removing metal ions from their respective salts. The popular reducing agents, such as hydrazine (N<sub>2</sub>H<sub>4</sub>), alcohol (C<sub>2</sub>H<sub>5</sub>OH), lithium aluminumhydride (LiAlH<sub>4</sub>), and sodium borohydride (NaBH<sub>4</sub>) were reported earlier.<sup>28–31</sup> Other chemical methods known as green synthesis methods use green solvents as a reductant obtained from green plants.<sup>32</sup> Previous studies have demonstrated the use of the chemical reduction process in green synthesis and the polyol synthesis methods.<sup>26,28</sup> Polyol methods utilize polyethylene glycol and polyvinyl alcohols to reduce metal ions into metal NPs.<sup>33</sup> The



Ashutosh Sharma

produced by powder metallurgy and additive manufacturing of titanium implant materials.

*Ashutosh Sharma works as an Assistant Professor in the Department of Materials Science and Engineering, Ajou University, Korea. He received his Ph.D. in Metallurgical and Materials Engineering from the Indian Institute of Technology (IIT Kharagpur), India. His research interests include micro-joining, metal matrix nanocomposites, electrodeposition and corrosion. Currently, he is working on high entropy alloys*

polymer may also serve as a capping layer that defines the size and shape of the resultant NPs. A similar process has been suggested by Schulman *et al.* where a microemulsion consisting of at least one polar and one non-polar solvent is mixed with a stable surfactant.<sup>34</sup> The surfactant forms the interfacial film that separates these two layers between the polar and the non-polar layer, producing microemulsions at this interfacial region. The example includes water or oil as a consequence of dispersing the oil drops into water.<sup>34</sup>

Powder metallurgy (PM) is another method that involves top-down and bottom-up techniques to obtain the resultant product. The first step is the milling of the powder particles down to nanoscale followed by their densification at high temperatures to achieve the bulk product. The milled nanopowder is subsequently densified by high temperature sintering (hot isostatic sintering, cold iso-static sintering, and spark plasma sintering (SPS)) methods to achieve bulk product.<sup>20</sup>

Laser ablation as a bottom-up method includes coating fabrication by heating, vaporizing, or sublimating a substrate by irradiating it with a laser beam. This technique has been beneficial over others because there is no need to evaporate the excess solvent that may be used in chemical methods.<sup>35</sup> Compared to other methods, laser ablation is faster, can produce easily controlled sizes and shapes, and has the possibility of mass production. Similarly, microwave processing is also a method where the sample is irradiated with a microwave source of energy.<sup>36</sup> When irradiated in the presence of a surfactant, the metallic salts decompose and lead to metal NPs.

### 3. Metallic and noble nanomaterials in biomedicine

Metal NPs are unique nanoscale materials that are easy to fabricate and manipulate. Owing to their powerful optical and electrical characteristics, metal NPs outperform their bulk counterparts. NPs' composition, shape, and size all play a role in their attractive physico-chemical properties. The confined electronic arrangement of metal NPs allows their use as a conducting element in the manufacture of special micro-, and nano-devices (e.g. single-electron tunnel diodes, nano-thermometers, etc.).<sup>37–39</sup> Amongst metal NPs, noble metal NPs play an important role in biomedicine, drug development, and imaging. Au, Ag, Pt, and Pd are the noble metal NPs that have received the most attention. Metal oxide nanoparticles (MOX), as well as common metals and transition metals able to conduct, e.g. CuNPs, CoNPs, NiNPs, SnNPs, and many others, have been used in the semiconducting packaging industry.<sup>40–43</sup>

Wet chemical methods make it simple to manufacture CuNPs, which have been extensively researched in the last few years. When preserved at normal temperature, CuNPs have excellent optical and catalytic characteristics, making them useful in biomedicine, optical imaging, and catalysis.<sup>44</sup> Due to their catalytic activity, Pt and PdNPs are also being studied. Photocatalytic and wet chemical reduction methods are simple synthesis techniques for producing catalytic NPs. Many indus-

trial catalytic coupling of C-C bond processes employ Pd-coated NPs as catalysts, including electroplating.<sup>45</sup> PdNPs are employed as membranes to filter hydrogen in some fuel-processing applications, as Pd is an outstanding hydrogen absorber.<sup>46</sup> Nanoparticles of Ni are also exciting as they play a major role in catalysis and magnetic storage. Most of these mentioned nanomaterials (including Au, Pd, Pt, Ag, etc.) have been extensively utilized in a broad range of biomedical application as photosensitizers. Particularly Au and Ag have appeared to be important materials due to high biocompatibility, ease of synthesis and surface functionalization, and ease of tuning of optical and physical properties. These novel metal nano-structures exhibit a variety of attractive characteristics, such as powerful light absorption, scattering, and localized surface plasmon excitations, which allow them to be used in outstanding biomedical applications.<sup>47</sup> Particularly the localized surface plasmon resonance (LSPR) property of metal nanomaterials is widely used for cancer treatment. Intriguingly, by modifying the size and shape of the nano-materials, the LSPR characteristics of novel metals can indeed be altered. The novel metal nanomaterial shows chemical and photostability which enables longer exposure time and a wide range of excitation energy. These properties allow the use of noble metals, particularly Au and Ag nanomaterials, in biomedical applications.<sup>47</sup> As per the field observations above, a wide range of Au and AgNPs have indeed been routinely used during medical applications. In the following sections, we will explore the different processes for novel Au and AgNPs synthesis and applications.

### 3.1 Gold nanoparticles (AuNPs)

The chemical element Au has an atomic number of 79 and an atomic weight of 197 g mol<sup>-1</sup>. A large quantity of gold is generally obtained from mining, and it has long been used for ornamental and decorative purposes. The melting and boiling points of Au are extraordinarily high: 1064 °C and 2807 °C, respectively. Even though it is a non-reactive substance, it may still be detected due to its high temperatures and electrical properties. It has found use in electronics and medicine too, in addition to its primary use.<sup>13</sup>

Michael Faraday's research of Au colloids in the nanoscale range is one of the earliest historical milestones in the nanoscience literature, from the middle of the 19th century. Colloidal Au is a suspension of nano-sized Au particles in a fluid, with remarkable optical characteristics. The visual, physical, and chemical characteristics of AuNPs are strongly influenced by their size.<sup>48</sup> AuNPs' size-dependent characteristics spurred a slew of scientists to investigate the relationship between size and shape.<sup>49</sup> AuNPs have been synthesized by chemical reduction methods in the desired size and shape for diverse applications. Spherical AuNPs, nanorods, AuNW, and nanocubes have a long history of study in the scientific literature. Spherical AuNPs are of particular relevance because of the ease with which they may be synthesized and the excellent yields that they provide.<sup>50</sup> AuNPs, as researchers know, are inert and excellently biocompatible materials that do not

oxidise easily. The chemical, optical, and electrical characteristics of AuNPs can be easily changed by manipulating surface morphology and surface functionalization. AuNPs were used in various bio-imaging application areas due to their unique localized surface plasmon resonance (LSPR) characteristics. The size and shape of AuNPs impact their photothermal conversion effectiveness generated by LSPR. The LSPR peaks can be tuned by adjusting the surface morphology of AuNPs including nanorods, nanostars, nanopyramids, and so on.<sup>47</sup> Jiang *et al.* used sodium borohydride (NaBH<sub>4</sub>) and sodium citrate (Na<sub>3</sub>C<sub>6</sub>H<sub>5</sub>O<sub>7</sub>) as a reducing agent as well as a capping agent to create AuNPs ranging in size from 5 to 50 nm. Furthermore, they studied the size-dependent photothermal conversion efficiency. They found that the photothermal conversion efficiency was increased from 65 to 80% when the size of AuNPs was decreased from 50.09 to 4.98 nm.<sup>51</sup> Yang and his co-workers employed a one-pot photoreduction process for the synthesis of poly(L-cysteine)-b-poly(ethylene oxide) copolymer gold nanoparticles. They stabilized the AuNPs with 62 ± 3 nm size by using a coating of a thin copolymer layer. The authors observed that the prepared NPs showed considerable near IR absorption with an impressive photothermal conversion efficiency of 62.1%.<sup>52</sup> Yang and co-workers prepared doxorubicin hydrochloride (DOX)/mesoporous silica NPs (MSN)-Au for chemo-photothermal synergistic therapy.<sup>53</sup> First, they prepared MSN by mixing cetyltrimethylammonium bromide (CTAB), sodium hydroxide (NaOH), and tetraethoxysilane (TEOS) in the aqueous medium. Furthermore, they functionalized MSN using (3-mercaptopropyl)trimethoxysilane to get MSN-NPs with a thiol group on the surface (MSN-SH). Secondly, they prepared AuNPs (~4 nm in size) by chemically reducing the HAuCl<sub>4</sub> using this Na<sub>3</sub>C<sub>6</sub>H<sub>5</sub>O<sub>7</sub> and NaBH<sub>4</sub> for delivery of drugs; MSN-SH nanoparticles were blended into the DOX solution, which is designated as DOX/MSN-SH. The DOX/MSN-SH nanoparticles were disseminated in phosphate-buffered saline water (pH ~7.4). Finally, 50 mL of NPs solution was then poured into DOX/MSN-SH, which is transformed into DOX/MSN-Au. Fig. 2 depicts the synthesis of mesoporous MSN-Au interconnected by Au-S bonds.

Their findings revealed that *in vitro* drug release was accelerated in the vicinity of glutathione (GSH) or near-infrared laser irradiation. This suggested that the DOX/MSN-Au system is an excellent candidate for redox-responsive and near-IR-triggered release of a drug. Pan and co-workers prepared Au nanorods using a seed-aided and surfactant-facilitated approach.<sup>54,55</sup> The schematic illustration of the synthesis procedure of Au nanorods is shown in Fig. 3a. The prepared Au nanorods were functionalized with TAT-type nuclear localization signals (NLSS). The electron microscopy (TEM) images of Au nanorods show that the average length and width are nearly 40.5 2.1 nm and 10.5 1.7 nm, respectively, as shown in Fig. 3b. The thiolated poly(ethylene glycol) and cysteine-containing TAT peptides were used as a surface modification. The aspect ratio of gold nanorods is approximately 3.9 nm, which has great significance for the efficient near IR-triggered photothermalysis process.

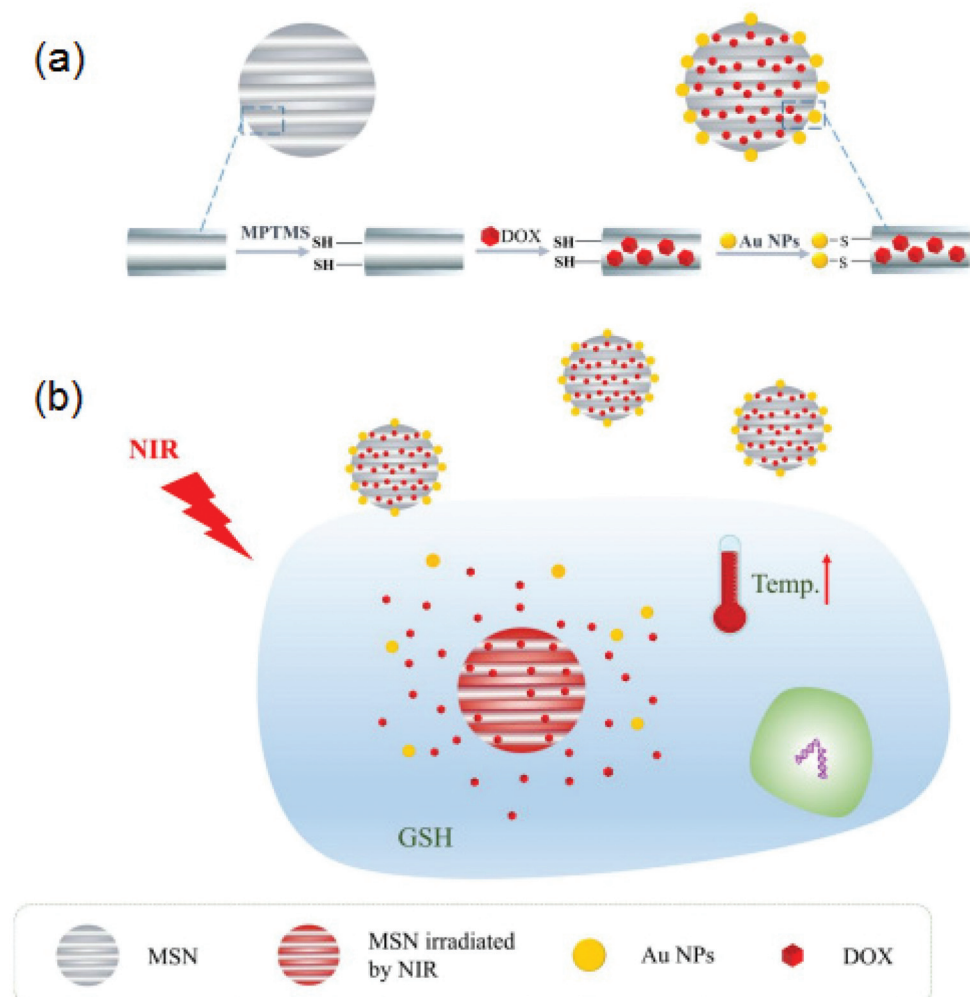


Fig. 2 (a) DOX/MSN–Au drug loading procedure and (b) redox responsive release of the drug with GSH, as well as the synergistic therapeutic effect of DOX/MSN–Au via chemo and photothermal therapy reproduced from ref. 53 with permission from [Elsevier], copyright [2021].

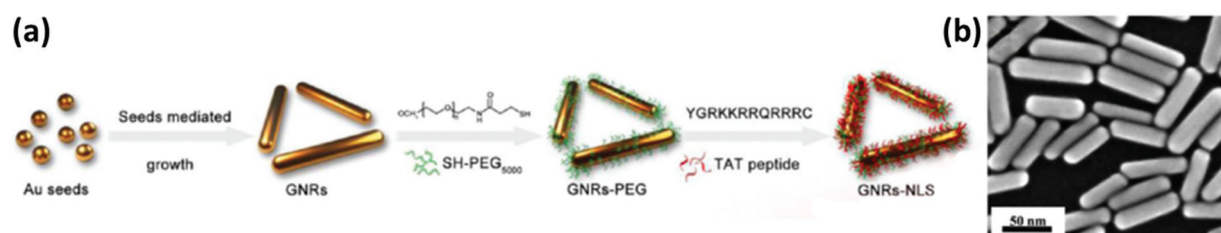
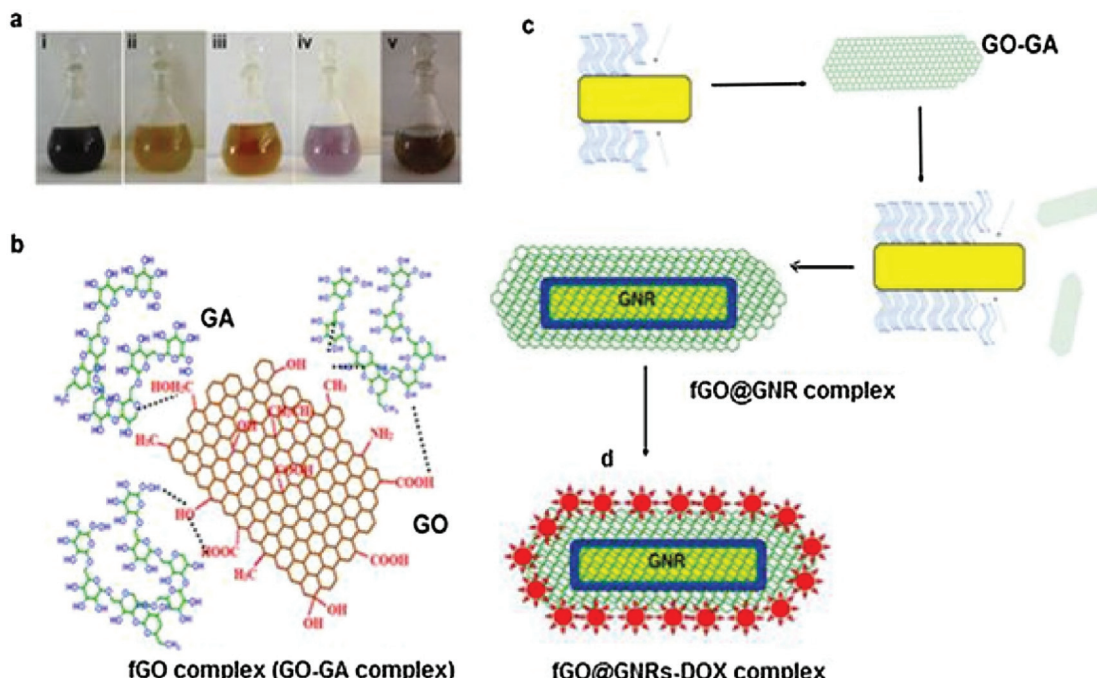


Fig. 3 (a) The technique for fabricating Au nanorods, and (b) the electron microscopy (TEM) images of Au nanorods, reproduced from ref. 55 with permission from [American Chemical Society], copyright [2017].

Khan and his collaborators created a nanocomposite of graphene oxide@Au nanorod for chemo and photothermal therapy.<sup>56</sup> They also investigated the release of doxorubicin in mice during tumor therapy. First, they used a modified Hummers technique to create graphene oxide (GO) followed by functionalizing it with a gum arabic layer (fGO-GA complex). The seed-mediated method was employed to produce a func-

tionalized (fGO) and Au nanorods (fGO-GNRs) conjugate. The processes for the production of GO and Au nanorods are depicted schematically in Fig. 4a-d. Furthermore, the fGO@GNRs-DOX conjugate was produced by coupling of DOX with previously produced fGO@GNRs. *In vitro* photothermal killing of A549 cells was used to study the kinetics of DOX discharge under near-IR illumination.



**Fig. 4** Major steps in the synthesis of the drug delivery vehicle based on GO and Au nanorods. (a) Reaction colors at different steps that lead to the formation of the final conjugates such as (i)–GO (ii) GA (iii) fGO (iv) fGO@GNRs and v–fGO@GNR-DOX; (b) fGO conjugate (GO–GA) synthesized after the reactions of GO with GA; (c) Incorporation of fGO in the GNRs (fGO@GNRs); and (d) anti-cancer medicine loading DOX on fGO@GNRs complex. Reproduced from ref. 56 with permission from [Elsevier], copyright [2021].

### 3.2 Silver nanoparticles (AgNPs)

Currently, due to their various unique physical and biochemical characteristics, silver (Ag)NPs are receiving a lot of attention. Their superiority is due primarily to the shape, structure, chemical composition, and crystal structures of AgNPs when compared to the bulk form.<sup>57–61</sup> Attempts have indeed been undertaken to investigate their appealing characteristics and use them in real-world antibacterial and anti-cancer therapeutic applications,<sup>62</sup> diagnostic and optoelectronic devices,<sup>63–65</sup> water disinfection,<sup>66</sup> and other pharmaceutical applications.<sup>67</sup> Despite the reality that silver as metallic particles possesses intriguing material characteristics and is a moderate and plentiful renewable resource, due to various aspects of their stability, such as oxidising in an oxygen-containing liquid, the application of Ag-based nanostructures has been restricted.<sup>68</sup> In a nutshell, compared to stable gold nanoparticles (AuNPs), AgNPs have untapped potential.<sup>59</sup> Prior investigation has evidenced that the physical, optical, and catalytic capabilities of Ag-NPs are heavily influenced by their size, dispersion, morphology, shape, and surface properties, all of which can be altered using various synthesis methods, agents such as sodium, and stabilizers.<sup>61,69</sup> Additionally, AgNPs are employed for antibacterial purposes due to the antibacterial property of Ag<sup>+</sup> ions. AgNPs' remarkable characteristics have permitted their application in nanomedicines, pharmacology, biosensors, and medical technology. Several studies have shown that AgNPs soak up electromagnetic visible and infra-

red wavelengths ranging from 380 to 450 nm, a process termed LSPR excitation. Park and coworkers<sup>70</sup> evaluated the optical properties of Ag nanoparticles of various sizes synthesised with gallic acid utilizing biological techniques. As per the research results, spherical Ag-nanoparticles (AgNPs) with a particle size of 7 nm have SPR at 410 nm, and those with a diameter of 29 nm have SPR at 425 nm. Moreover, 89 nm AgNPs have a broader band with a maximum resonating wavelength of 490 nm. The breadth of the SPR banding was shown to be related to the sizes of NPs. For example, Lee *et al.* investigated the dependencies in the sensitivities of SPR response (frequency and band) that allowed NPs to detect changes in their surroundings.<sup>71</sup> Substantial improvement in the amplitude and sharpness of the surface plasmon band was found in nanorods with higher Ag content, which might lead to improved sensing precision even with comparable plasmon responsiveness. As a result, when compared to AuNPs, Ag-nanorods have the benefit of being superior scatterers.

Fig. 5 shows the shape and size of Ag nanoparticles which exhibit peak wavelengths in the range 400–850 nm. The SPR band is shown in Fig. 5a.<sup>72</sup> The absorption spectra of Ag nanoparticles as measured by visible spectroscopy demonstrate the modulation of shape and size of Ag nanoparticles by color scattering (Fig. 5b).<sup>73</sup>

Two main challenges in AgNP-based nanoparticles are nanotoxicity and the environmental implications of AgNPs on a nanometer scale. To anticipate the potential cytotoxicity of AgNPs, it is important to examine the phase transition that

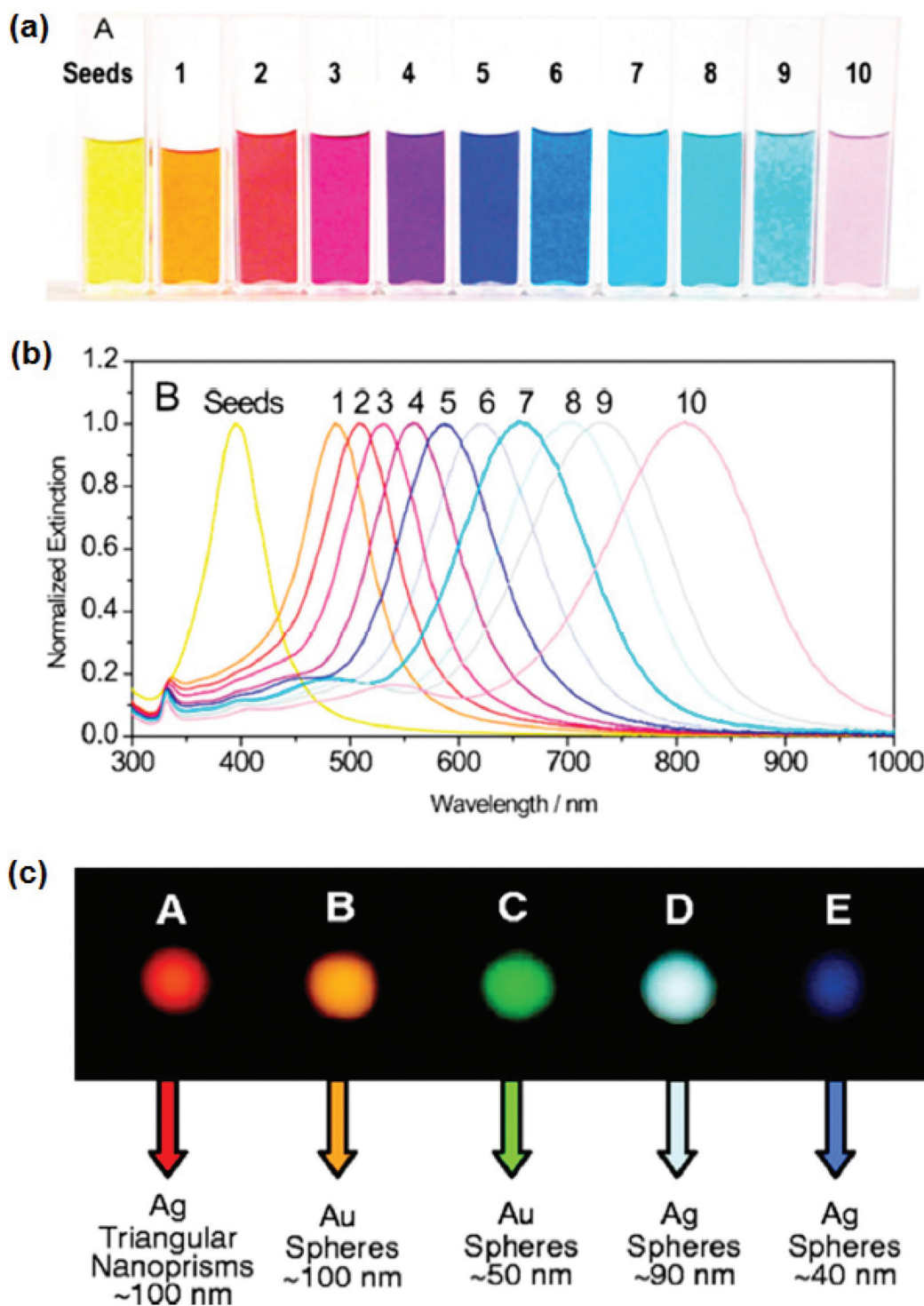


**Fig. 5** (a) Photograph and (b) optical spectrum of Ag nanoprisms. The ability to tune the plasmon resonance all across visible and near IR regions of the spectrum is enabled by the control of the edge length of nano prisms. Reproduced from ref. 72 with permission from American Chemical Society [2008]. (c) Dark-field microscopy of Ag and Au nano prisms. The spheres (left to right) illustrate the tunability of the scattering color of AgNPs based on their size and shape. Reproduced from ref. 73 with permission from [Science], copyright [2021].

happens as AgNPs pass through into the intracellular surroundings.<sup>68</sup> The utilization of AgNPs as powerful anticancer or antibacterial agents has drawn a lot of attention based on

their chemical cytotoxic characteristic. Despite many ideas, the mechanism of AgNPs' antibacterial activities has yet to be thoroughly confirmed. The potential cytotoxic mechanism can

be summarized based on a literature review as follows: (i) AgNP adherence to the microbial cell membranes, altering the lipid bilayer and enhancing the cell membrane; (ii) AgNP intracellular penetration; (iii) the toxicity of AgNP on cells caused by the generation of reactive oxygen species and free radicals, which cause damage to intracellular organs (*i.e.*, mitochondria, ribosomes, and vacuoles) and biomolecules such as DNA, proteins, and lipids; and (iv) modulation of intracellular signal transduction pathways in the direction of apoptosis.<sup>74</sup> Ion release and surface area as well as charge, concentrations, and colloid state can influence the cytotoxic effects of AgNPs. Ag ions can bind to thiol groups in crucial bacterial enzymes and proteins, causing harm to cell respiration and inducing apoptosis. An additional method of AgNPs inducing cell death is the production of reactive oxygen species (ROS) and free radicals, as depicted in Fig. 6.

AgNPs' cytotoxicity is primarily owing to their ability to generate ROS species as well as free radical components such as  $O_2$ ,  $H_2O_2$ , OH, HOCl, and superoxide anions.<sup>75</sup> When free radicals interact with bacteria, they disturb the integrity of the cell wall, which results in cell death.<sup>63</sup> AgNPs can also grow on the cell membrane of bacteria and penetrate it, resulting in structural alterations to the membrane or increasing its permeability, which all induce cell death. Surprisingly, the

potency of AgNPs antibacterial properties is connected to different kinds of bacteria species, including Gram +ve and -ve bacteria. This is an attribute of variations in the design morphology and width of different cell walls.<sup>76</sup> Gram-negative bacteria, such as *E. coli*, are more sensitive to Ag<sup>+</sup> ions than Gram-positive bacteria, including *S. aureus*.

The variation in activity is attributable to the peptidoglycan that is an essential element of bacterial membranes. Gram +ve bacteria have a cell membrane that is made of a negatively charged peptidoglycan layer that is around 30 nm wide, and Gram-negative bacteria have such a peptidoglycan layer that is only 3 to 4 nm thick.<sup>77,78</sup> Loo *et al.* tested Ag and curcumin nanostructures against Gram +ve and -ve microbial species and discovered that 100 g mL<sup>-1</sup> NPs can disrupt established biofilms. This formulation's long-lasting antibacterial properties can be used in antimicrobial therapy.<sup>79</sup> Paril *et al.*<sup>80</sup> studied the antifungal effects of AgNPs and Cu nanospheres on timber-rotting fungus. The AgNP therapy needed a relatively small amount of NPs and showed great efficacy over *T. versicolor* fungus in contrast to *P. placenta* fungi, demonstrating that AgNPs had different antifungal actions against white and brown rot fungus, respectively. The specifics of antibacterial characteristics are outside the focus of this investigation and have been discussed elsewhere.<sup>62,67,81</sup>

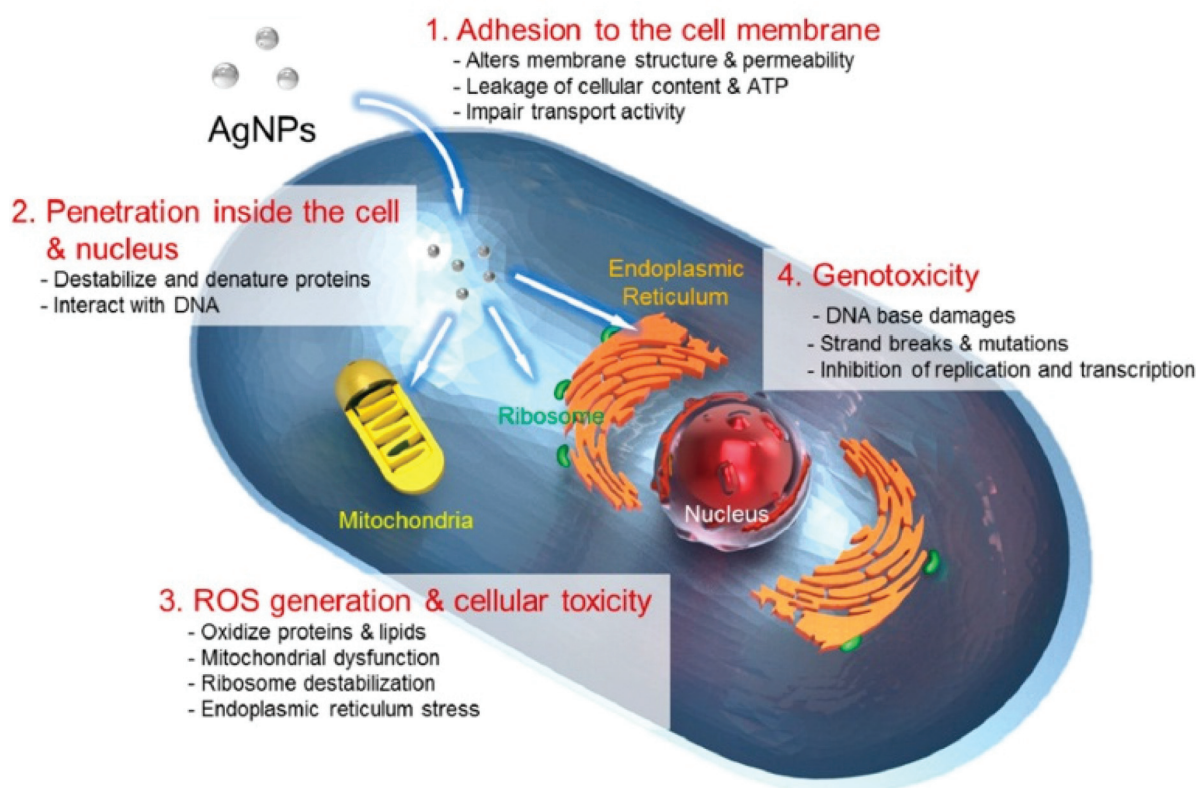


**Fig. 6** Cytotoxic mechanisms of AgNPs. (1) Adherence of AgNPs to the cells rupturing the cell membrane and modifying mass transport, (2) inside-cell interaction of AgNPs and Ag ions to cell components (organelles and biomolecules) and modulation of the cell function, (3) production of ROS through AgNPs and Ag ions on the inside of the cell causes cellular damage, and (4) onset of genotoxicity by AgNPs and Ag ions. Reproduced from ref. 74 with permission under CC By 4.0 license [2019].

## 4. Magnetic nanoparticles (MNPs) in biomedicine

Although there are several pure phases of oxides in natural deposits, the most often used MNPs are nanoscale zero-valent irons,  $\text{Fe}_3\text{O}_4$ , and  $\text{Fe}_2\text{O}_3$ . MNPs have a range of physicochemical characteristics due to differences in their Fe oxidation states and their capacity to remove contaminants. Amongst them, the most popular  $\text{Fe}_3\text{O}_4$  is a black ferromagnetic oxide that usually contains both  $\text{Fe}(\text{II})$  and  $\text{Fe}(\text{III})$ . The existence of the  $\text{Fe}^{2+}$  state makes it an excellent e-donor and it is used in magnetic storage. Fig. 7 depicts the many magnetic conditions that occur during the crystallization of iron.<sup>82,83</sup>

The paramagnetic crystal generates magnetization that is arbitrarily aligned, and the entire structure has no net magnetism. Whenever a paramagnetic state is subjected to an exterior magnetism, the moment aligns resulting in minor net crystal magnetism. The individual magnetic moments are arbitrarily aligned in the ferromagnetic and antiferromagnetic state in the absence of external magnetic field, as seen here (Fig. 7). Bulk ferromagnetism has many magnetic domains with evenly magnetized areas. Each domain is discretized by a non-uniform magnetization dispersion (domain walls) with a unique magnetization vector. Because the vectors of each region are not aligned, the net magnetic moment is minimal. Many magnetic particle processes depend on the use of magnetic fields to change their features, which are dependent on the effectiveness of the particulate magnetization as well as

the field gradients.<sup>85</sup> Because of their tiny radius and magnetization, single-core super-paramagnetic nanoparticles are less efficient when subjected to force. However, in the context of multi composites, the produced magnetic field lines are good enough to allow magnetic targets with low field strength and steepest decent value to be used.<sup>86,87</sup> The interactions of a magnetic dipole-dipole and a dipole field would result in the cluster and the generation of rather large micrometer-sized longitudinal aggregates, resulting in a dramatic drop in effective surface area and possible blockage of a blood cell. As stated previously, bulk ferromagnetism comprises multiple domains with uniformly magnetic sections. Table 1 lists significant advancements in polymer-dressed MNPs for the biomedical field.<sup>84</sup>

As the size of the magnetic particles goes down, domain size and density reduce until a single domain remains underneath the critical particle diameter ( $\approx 15\text{--}20\text{ nm}$ ) that produces superparamagnetic metal oxide NPs.<sup>83,95,96</sup> Superparamagnetic metal oxide nanoparticles have piqued the interest of researchers owing to a couple of desirable properties, biocompatibility and easy fabrication. Additionally, no hysteresis is generated, leading to zero residual magnetism (Fig. 7). This characteristic aids in preventing coagulation, which reduces the probability of aggregation *in vivo* in contrast to certain other MNPs.<sup>97</sup> The most well-known implementations of MNPs in biomedicine are in MRI as contrast media.<sup>98–101</sup> The influence of physical characteristics and the importance of physicochemical characteristics in determining the efficiency of targeted delivery

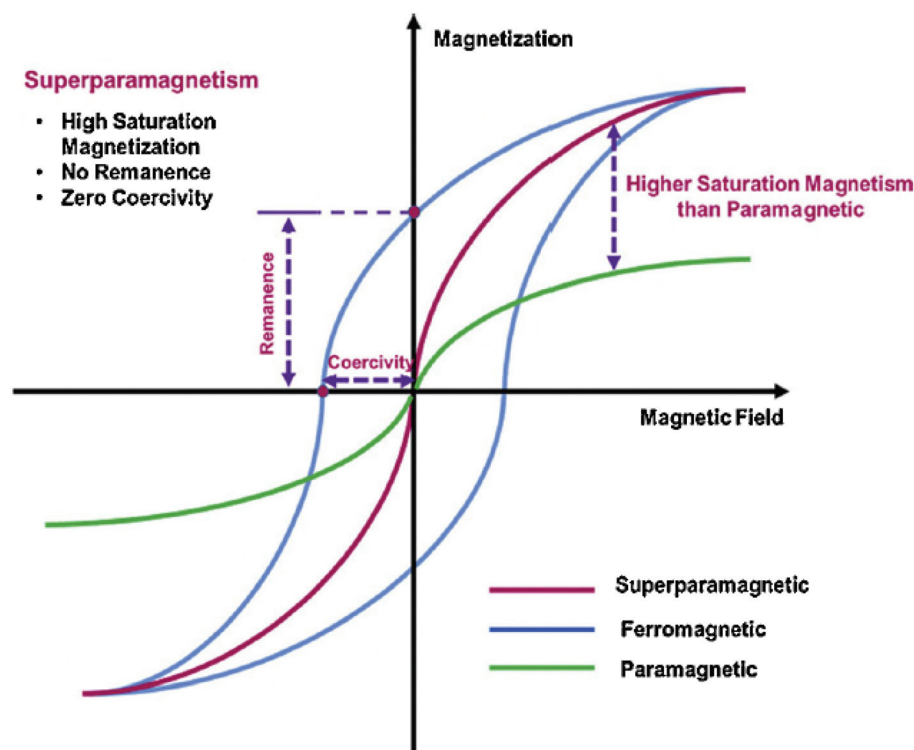


Fig. 7 Magnetic properties of ferromagnetic materials. Reproduced from ref. 84 with permission from [Elsevier], copyright [2017].

**Table 1** Recent progress in polymer decorated MNPs for biomedical applications

Hybrid polymer MNPs	Applications	Ref.
Chitosan functionalized $\text{Fe}_3\text{O}_4$ doped rare earth nanoparticles	Paclitaxel (PTX) drug delivery for lung cancer	88
Gly-copolymer-modified mesoporous silica MNPs	Drug delivery and magnetic resonance imaging (MRI)	89
MNPs coated with 3-methacryloxypropyl trimethoxysilane and polymerized with glycidylmethacrylate-grafted maleated cyclodextrin	Controlled delivery of anticancer 5-fluorouracil drug	90
Gold nanoparticle hybrid MNPs	DOX anti-cancer drug delivery with precision	91
RGD peptide functionalized polyethylene glycol-coated magnetic hydrogel.	Targeted delivery of the anti-cancer DOX drug	92
MNPs made of $\text{Fe}_3\text{O}_4$ -carboxymethyl chitosan hybrids	Rapamycin is selectively supplied to tumours.	93
<i>N</i> -Glycrrheticinacid/polyethylene glycol/chitosan/MNPs	Targeted brucine delivery <i>via</i> hepatocytes and mitochondria (natural anticancer drug)	94

cannot be overstated. Usually, MNPs must overcome biological obstacles to reach their intended target: physical and physiological barriers.<sup>102</sup> Shape, size, surfaces' qualities, and magnetic properties are the primary factors that govern their behavior *in vivo*.

## 5. Carbon nanostructures in biomedical applications

Graphene, the 'miraculous material', is a 2D structure of paper of  $\text{sp}^2$ -hybridized carbon atoms arranged in a hexagonal honeycomb lattice (Fig. 8a). In the beginning, a few layers of graphene were gently exfoliated from graphite, demonstrating enormous potential in the disciplines of materials engineering, physics, chemical, biology, and many others.<sup>103–107</sup> Following other types of carbon nanocrystal, such as fullerene (which would be formed by trying to wrap 2D graphene into a 0D molecule, Fig. 8b), carbon nanotubes (CNTs, formed by cylindrically rolling 2D graphene layers into 1D nanotubes, Fig. 8c), and graphite (2D graphene sheets are stacked into

structures, Fig. 8d), the occurrence of graphene has reopened a few interesting new disciplines in engineering.

Due to the obvious pinching off of the transport and valence bands at the Brillouin zone corner, charge carriers in graphene, for instance, interact like massless relativistic particulate or Dirac fermions, resulting in a linear distribution of the wavelength range.<sup>108</sup> The metal-like behavior may be adjusted to a semiconducting character by generating graphene nanoribbons of variable size. Based on electron confinement phenomena, graphene nanoribbons with a width less than 10 nm showed semiconductor capabilities, but for wider width, the characteristics are primarily reliant on the edge configuration.<sup>109</sup> Furthermore, remarkable electrical conductivity (charge carriers mobility  $\approx 2 \times 10^5 \text{ cm}^2 \text{ V}^{-1} \text{ s}^{-1}$ ) is seen in graphene due to  $\text{sp}^2$  hybridisation of carbon atoms.<sup>110,111</sup> At ambient temperatures, graphene also demonstrated the unique partially quantum Hall effect for both holes and electrons.<sup>112</sup> It also has some superior mechanical strength (nearly 200 times stronger than steel) and other characteristics (Young's modulus  $\approx 1100 \text{ GPa}$ ), ultra-thin nanostructure ( $10^6$  times thinner than a human hair), very high surface area ( $\approx 2630 \text{ m}^2 \text{ g}^{-1}$ ), superior heat conductivity ( $\approx 5000 \text{ W m}^{-1} \text{ K}^{-1}$ ),

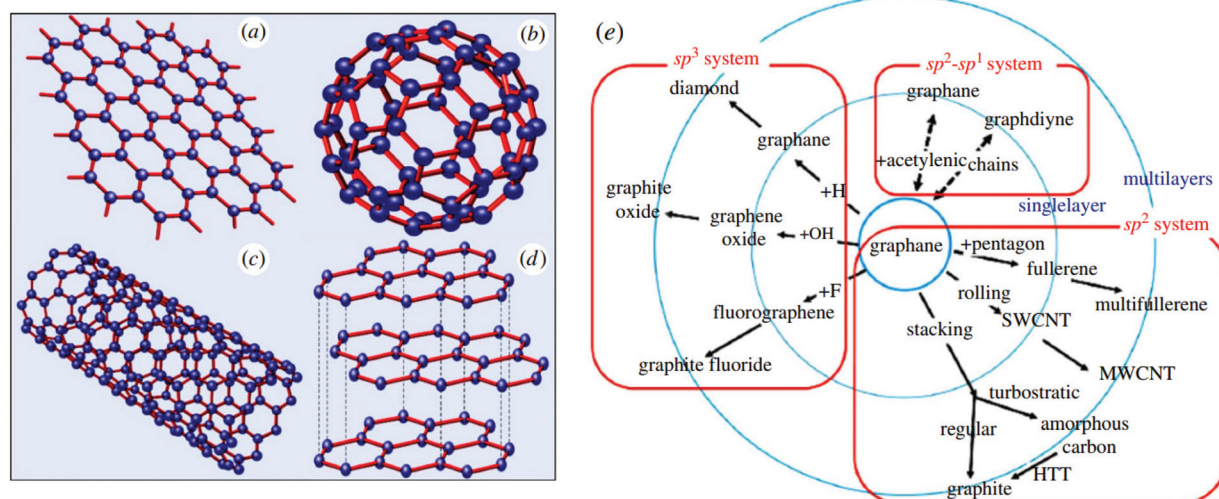


**Fig. 8** Schemes for graphene structure. (a) 2D graphene layer, (b) 0D fullerene, (c) 1D carbon nanotubes, (d) 3D graphite, reproduced from ref. 103 with permission from [IOP Publishing], © IOP Publishing 2006, and (e) graphene derivatives reproduced from ref. 104 with permission from [Royal Society of Chemistry], copyright [2014].

high stretchability, full flexibility but high insulative properties, inherent biocompatibility, and chemical inertness.<sup>103–107</sup> Furthermore, the latest advancements in new materials, cost-effectiveness, and scalable manufacturing technologies have enabled it to become one of the most appealing nanomaterials in different fields such as microelectronics, composites, alternative energy, sensor systems, and catalysts supports.<sup>113–115</sup> Due to these aforementioned characteristics, and its biocompatibility, functionalized graphene has been applied in chemical and biological applications,<sup>116–118</sup> a few of which include biosensing, antibacterial/antiviral interaction, anti-cancer interaction, photothermal treatment therapy (PTT), targeted pharmaceutical administration, electrical stimulation of cells, and tissue culture.<sup>119–130</sup>

### 5.1 Graphene derivatives for bioimaging

Researchers have found that graphene and its derivatives have garnered sufficient attention for biological applications when compared to their non-medical benefits. Fig. 9a illustrates that graphene derivatives have nearly 63% biological uses, compared to 37% non-medical uses.<sup>131,132</sup> Fig. 9b illustrates the extensive biological uses of graphene-based materials in various important disciplines.

Because of graphene and its derivatives' distinct chemical, electrochemical, optical, electrical, and electronic properties, as well as bio-functionalizations of graphene-based nanomaterials with various biomolecules and cells, and their increased biocompatibility, solubility and selectivity, graphene and its derivative products show some intriguing applications in optical/electrochemical devices, bioimaging, electronic items, spectrometry, and a variety of other fields.<sup>133</sup> For example, a graphene-derived or oligonucleotide noncomplex is used as a framework for *in vivo* sensing of biomolecules, DNA detection techniques, bimolecular imaging in live cells, protein detection, heavy metal and pathogenic sensing, and so

on. In terms of an *in vivo* sensor of biological molecules, graphene field effect-transistor derived sensors have been extensively researched for the identification of nucleic acids, proteins, *etc.*, and growth regulators have indeed been conclusively proved by using appropriately functionalized ultrathin derivative products to nucleic acid aptamers and carbohydrates for tracking target-specific changes in electric signals to quality handset ratio.<sup>121,130,132,134–137</sup> Fig. 10a depicts a schematic view of the detecting of vascular endothelial growth factor (VEGF) using N-doped graphene field-effect transistor (FET) sensors.<sup>135</sup> Further, anti-immunoglobulin G is connected to a TRGO surface by AgNPs and acts as the specific recognition site for IgG coupling, as shown in Fig. 10b.<sup>136</sup>

Graphene FETs have emerged as a promising tool for biosensing and analysis as a result (such as DNA hybridization, hormonal catecholamine molecules, protein binding events, heavy metals, *etc.*). Previous authors have demonstrated the method of fluorescent-tagged DNA interaction with bi-functional graphene for DNA detection and monitoring, where both single-stranded (ss) and double-stranded (ds) DNA is collected onto graphene sheets. Because ssDNA interacts more vigorously than dsDNA, the fluorescence on ssDNA deteriorates even more, and biosensing improves. Complementary DNA can be displaced from graphene sheets when it comes close to the adsorbed ssDNA. Moreover, the deposited DNA on graphene is protected from enzyme degradation, enhancing sensor performance.<sup>137</sup>

Owing to graphene's aromatic system and capacity to hold diverse ionic components onto its basal planes (which contributes to the unique capability to absorb bio-molecules), graphene derivatives may become efficient biosensors in the near future. In bio-imaging, a nanohybrid of graphene with fluorescent molecules is employed as a fluorescent cellular imaging probe *in vitro* and *in vivo*.<sup>138</sup> Fig. 11a shows that

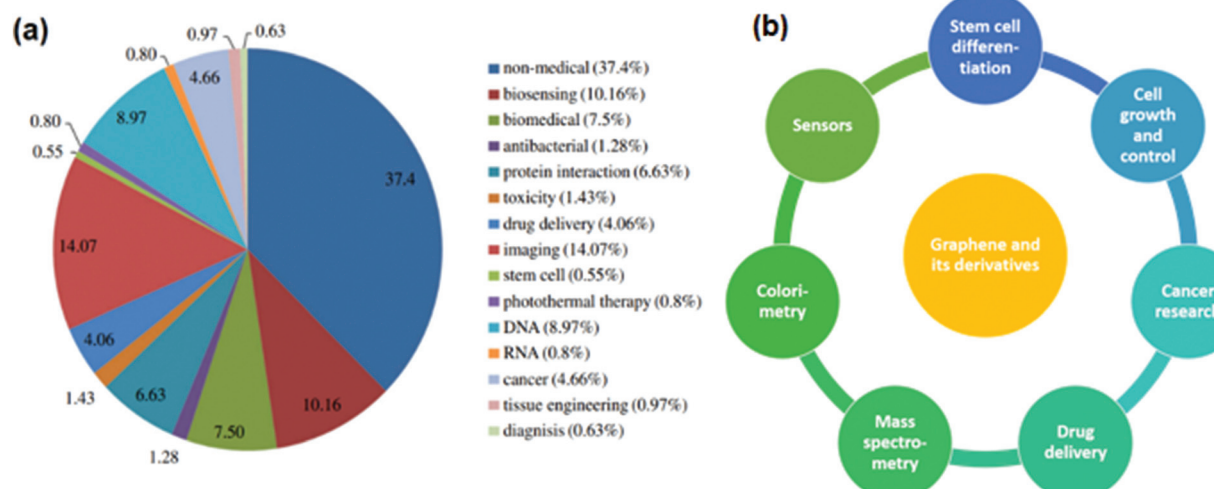


**Fig. 9** (a) Biomedical applications of graphene derivatives, reproduced from ref. 131 with permission from [American Chemical Society], copyright [2013], (b) important fields of biomedical applications of graphene derivatives.

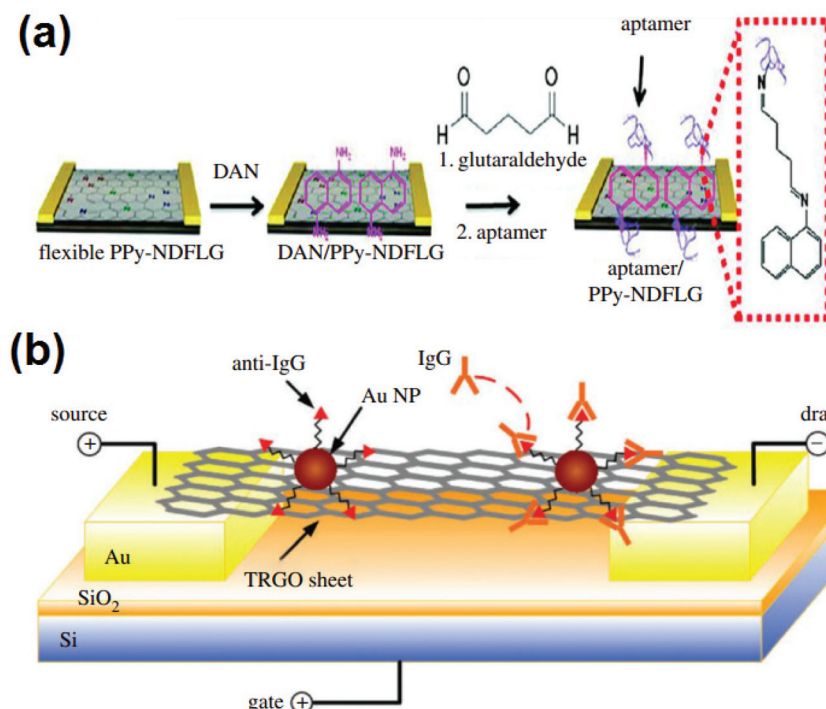


Fig. 10 (a) Illustration of N-doped graphene FET biosensor for detection of VEGF, reproduced from ref. 135 with permission from [Wiley-VCH], copyright [2012], (b) graphene FET schematic for detection of protein high binding occurrences, reproduced from ref. 136 with permission from [Wiley-VCH], copyright [2010].

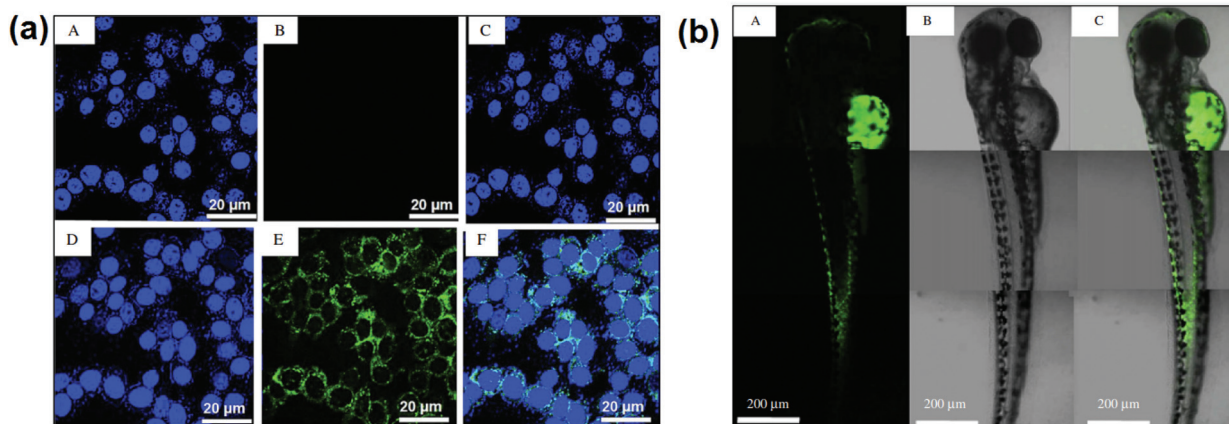


Fig. 11 (a) *In vitro* CSLM images of HeLa cells under control (top row) and treatment (bottom row, incubated with  $20 \text{ mg ml}^{-1}$  of MFG for 24 hours) conditions. In all of the images, the nuclei of HeLa cells were stained with DAPI blue dye. A DAPI filter was used to obtain the nucleus images in (A) and (D). A FITC filter was used to capture MFG's green fluorescence in (B) and (E). (C) and (F) are overlays of the stained nucleus and MFG fluorescence, respectively. (b) CSLM images of MFG distributed in a fully grown (72 hpf) zebrafish (A) fluorescence image of MFG with a FITC filter, (B) DIC image, and (C) overlay image, reproduced from ref. 138 with permission from [Elsevier], copyright [2012].

multi-functional graphene (MFG) can be used as a bio-degradable imaging probe after *in vitro* cytotoxicity testing on HeLa cells. Fig. 11b exhibits *in vivo* pictures of zebrafish treated with fluorophore MFG, and the investigation indicates no major abnormalities, nor does it impact the survival rate following MFG microinjection. MFG is only released into the cytoplasm of zebrafish and shows good co-localization and

biodistribution from the head to the tail, according to confocal laser-scanning microscopy (CLSM).<sup>138</sup>

Furthermore, without even any surface preparation or functionalization techniques, the photoluminescent properties of graphene quantum dots (GQDs) have been explored for internal monitoring. In fact, N-doped GQDs are now being evaluated as a bioimaging material, with N-GQDs being

injected into HeLa cells to demonstrate their bioimaging quality utilizing confocal microscopy.

As can be seen in Fig. 11a, strong green fluorescence is detected within the cells (A, B, C, D, E, and F) demonstrating that the N-doped GQDs have now been internalised by the cell lines and are predominantly found in the cytoplasm, implying that they could be employed as a bioimaging probe.<sup>139</sup> Furthermore, the GO-MNPs composite is used to enhance the MRI signal for *in vivo* and non-invasive cellular imaging.<sup>140,141</sup> Fig. 11b illustrates the conjugation of aminodextran-coated  $\text{Fe}_3\text{O}_4$  MNPs with GO (A, B, and C), accompanied by cellular absorption and subsequent MRI.<sup>140</sup> Furthermore, antibody-coupled GO has been utilized in positron emission tomography (PET) for tumor cells (Fig. 11c).<sup>142</sup>

Electrochemical sensors containing bio-macromolecules, enzymes, and molecules (such as hydroxyl radicals, nicotinamide adenine dinucleotide ( $\text{NAD}^+$ ), dopamine, glucose, and others) that used a nanohybrid (graphene/GO/reduced GO-metallic/organometallic complex) also have attracted a lot of interest.<sup>143–145</sup> For example, using the differential pulse voltammetry approach, direct electrochemical DNA sensors based on AuNPs/graphene film have been created. It has also been discovered that the accepted immobilization-free biosensor can distinguish between single- and double-misaligned DNA. The advantage of this electrochemical process is that it is more environmentally friendly and faster, and unlike chemical reduction it does not contaminate the reduced material. It can also lower the oxygen functions of the GO more effectively at very negative potential.<sup>143</sup>

In mice, Ang *et al.* used graphene FET arrays on quartz to detect malaria-infected red blood cells (RBCs). The incorporation of graphene FET arrays into a microfluidic channel results in the 'stream' detection of malaria-infected RBCs. The electrode was shielded by SU-8 photoresist that also serves as the sidewall of the microfluidic channel through which cells move. Infected RBCs produce highly sensitive capacitive changes in graphene conductivity. As a result, infected RBCs could be easily identified by analyzing the difference in conductance.<sup>146</sup>

Interfacing graphene derivatives with micro-and nano-materials also contributes to the construction of certain biosensors for the detection of DNA, protein, and pH. Even though the bulk of both the graphene-based medical applications described above include pure graphene, GO, and reduced GO, certain freshly produced graphene derivatives have also been found to have fascinating and unique uses in biomedicine. Graphdiyne, for instance, demonstrated promising amino acid detection performance and has the potential for biosensing applications. When the quantum electrical conduction properties of graphdiyne–amino acid complexes are compared to those of pure graphdiyne, it appears that the amino acid molecules may produce distinct alterations in graphdiyne's electrical conduction.<sup>147</sup> Similarly, graphone, semi-hydrogenated graphene with only one face of the C=C bonds saturated with hydrogen, on either hand, is a very well-magnetized semiconductor.<sup>148</sup> Because of the coexistence of

ferromagnetic materials and ferromagnetism, hydroxylized graphene, which is produced by having to replace the H atom on graphene with –OH, is multiferroic. As a corollary, graphene derivatives have been used in organic ferroelectrics,<sup>149</sup> bringing up interesting possibilities in the realm of molecular ferroelectricity, which now has fascinating links to biological ferroelectricity.<sup>150</sup> Similarly, graphane, completely hydrogenated graphene, has demonstrated superior biosensing capabilities than graphene or may be used in new biosensing devices. When compared to conventional graphene, graphane has demonstrated distinct electrochemical behavior in the context of oxidation or reduction of key biomarkers, also including ascorbic acid, dopamine, and uric acid.<sup>151</sup>

## 5.2 Fullerenes, carbon nanotubes (CNTs), nanodiamonds (NDs), and carbon dots (CDs) in biomedicine

Owing to their distinctive properties, carbon nanotubes (CNTs), fullerenes, nanodiamonds (NDs), and carbon dots (CDs) have been widely explored in the fields of electronics, optics, renewable energy, and healthcare. The distinction in shape properties arises due to the atomic hybridization ( $\text{sp}$ ,  $\text{sp}^2$  or  $\text{sp}^3$ ) of C-atoms (Fig. 12). The structures of CNTs, fullerenes, NDs, and CDs are shown in Fig. 12. The different physicochemical characteristics of various nanomaterials, including such electrochemical and redox potential, impact their biological activities.<sup>152–155</sup> Buckminsterfullerene (C<sub>60</sub>), which has 60 C atoms as well as a distorted icosahedron containing 20 hexagons and 12 pentagons and resembles a football in appearance, is amongst the most researched of carbon nanostructures.<sup>156</sup> The C<sub>60</sub> molecule has a diameter of roughly 1 nm.<sup>157</sup> There are two main methods for making fullerenes: top-down and bottom-up (through lasers or heat-

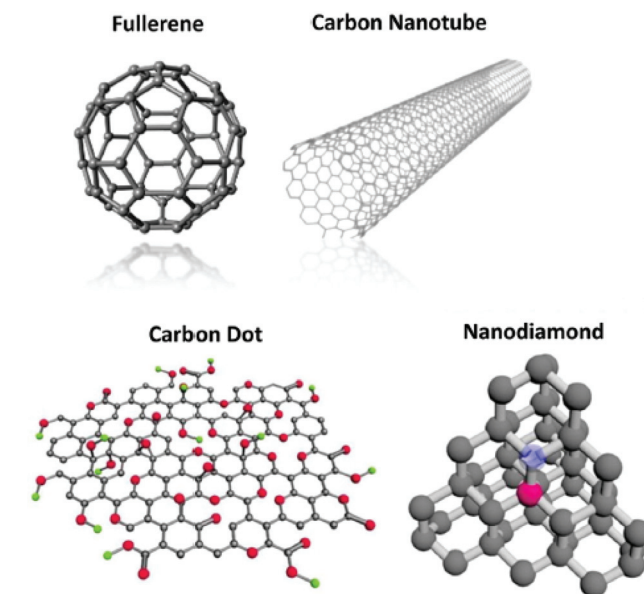


Fig. 12 Different forms of carbon nanostructures (fullerenes, CNTs, CDs, NDs) reproduced from ref. 158 with permission from [American Chemical Society], copyright [2015].

induced evaporation of graphite),<sup>157–159</sup> and a bottom-up approach (direct chemical synthesis from smaller aromatic precursors).<sup>160</sup> Furthermore, its ultrasmall size, homogeneous dispersity, and adjustable chemical alterations are gaining traction in biomedical investigation, particularly in medicines, diagnostics, and biomedical image analysis.<sup>158,161</sup>

CNTs are 1D large molecules made up of one or many coaxial tubes of the graphitic sheet. They are primarily categorized into two kinds: SWCNTs, which are made up of a single graphitic sheet, and multiwalled CNTs (MWCNTs), which are made up of several coaxial graphitic layers. The carbon arc-discharge approach, the beam method, and the CVD technique are the three major ways for producing CNTs.<sup>162,163</sup> Because of their unique chemical, structural, mechanical, optical, and electrical characteristics, CNTs are an intriguing choice for biological study.<sup>164</sup> Owing to their high aspect ratio and multi-functional surface features, CNTs have good drug delivery potential. SWCNTs also show remarkable optical characteristics due to the presence of the bandgap in semiconductive SWCNTs, which has led to their usage in photothermal and photodynamic treatments.<sup>165–167</sup> Meanwhile, CNTs are intriguing materials for tissue engineering because of their excellent flexibility, strength under mechanical strain, and biocompatibility.<sup>168–171</sup> Hydrophobic carbon nanotubes can be converted to water-soluble CNTs, which are less toxic and more biocompatible than untreated CNTs.

NDs are carbon particles with diameters ranging from 2 to 8 nm and a faceted truncated octahedral architecture.<sup>172</sup> The core of NDs is  $sp^3$  hybridized, whereas the surface defect sites are  $sp^2$  hybridized.<sup>173,174</sup> Detonation NDs and high-pressure, high-temperature NDs are two types of NDs that are commonly used in biomedicine. Detonated NDs are produced by the decomposition of highly explosive mixtures using negative oxygen balance in inert gas or coolant.<sup>174,175</sup> Further purification is needed to filter out the NDs amongst other allotrope mixtures as impurities. NDs have a high surface oxygen content (primarily carboxyl groups), which encourages better surface potentials and aqueous colloidal dispersions without additional functionalization.<sup>156</sup> It has been reported that NDs can be rapidly eliminated from the lungs and gradually eliminated from the spleen, liver, and kidney over 10 days.<sup>172</sup> However, CNTs had long-term retention and led to fibrosis and pulmonary toxicity.<sup>176</sup> Surface functionalization of carbon compounds increases their efficacy for several drug delivery and imaging techniques, which widens their scope for biomedical applications.<sup>177,178</sup>

## 6. Core applications of carbon nanostructures in therapeutics

Because of their desired size range, significantly higher surface area, adjustable surface chemistry, and the possibility of slow release, newly functionalized carbon nanomaterials have good drug loading, excellent biocompatibility, and remarkable pharmaceutical effectiveness. Carbon nano-

materials can also be functionalized with a wide range of medicines, such as chemotherapeutic medications, bioactive peptides, proteins, and acids.

### 6.1 Chemotherapy drugs

Cancer is a diverse illness, and various patient groups may respond to the same treatment combination in drastically different ways.<sup>177</sup> Notably, because of the improved permeability and retention (EPR), carbon nanomaterial delivery may achieve comparable efficacy with substantially lower dosages compared to traditional chemotherapy medicines, therefore minimizing the related adverse effects produced by chemotherapy treatments. Overcoming medication efflux-based chemoresistance is among the most common applications of carbon nanomaterials. Among them, the ABC transporters (ATP-binding cassettes transporter) induce a common mechanism of drug-resistant since numerous ABC transporters are capable of effluxing drug molecules, notably anthracyclines.<sup>179–181</sup> Diverse studies have been done on the ND–anthracycline complex, which somewhat improved anti-tumor efficacy but also reduced the harmful side effects caused by anthracyclines.<sup>172,182–185</sup> In this case, NDs sequestered the active molecules for a longer period than the medication alone, reducing effectiveness during the initial period. These ND–drug complexes, on the other hand, have a delayed but time-controlled or sustained drug-release, that also increased overall effectiveness throughout therapy.<sup>179</sup> In addition to solid tumours, ND-based administration has been utilized to treat chemoresistant leukemia, with improved effectiveness compared to daunorubicin individually, by circumventing efflux systems.<sup>186</sup> Surprisingly, anti-angiogenic junctions have indeed been discovered in NDs which limit tumour formation, making NDs a viable anti-cancer drug.<sup>152,187</sup>

Functionalized fullerenes are also useful nanocarriers for chemotherapeutic medicines due to their optimum sizes and hydrophobic surface characteristics. Fullerenes can quickly pass cell membranes, which is a significant benefit.<sup>178,188</sup> Some chemotherapeutic medicines (e.g., PTX and DOX) are complexed with C60 upon this surface of the cell. The pH-sensitive release mechanism is related to the significant toxicity in HeLa cells, indicating their potential for killing cancerous cells.

The distinctive architectures and functional surfaces of CNTs have been considered a potential medication delivery pathways.<sup>178,189</sup> Various compounds with accessible functional groups could be coupled to the modified CNTs. Hydrophobic drugs, on the other hand, can be bound to CNTs through – stacking or hydrophobic interaction. PTX was effectively covalently bonded to SWCNTs, and SWCNT-PTX had excellent solubility and long blood circulation, while exhibiting comparable toxicity to Taxol. Additionally, *in vivo* cancer therapy exhibits a substantial reduction of tumour development with few negative impacts.<sup>190</sup> DOX, as a chemotherapeutic medication, was loaded into CNTs and exhibited up to 4 g DOX per 1 g of SWCNTs *via* – stacking.<sup>191</sup> The circulatory system duration of

the CNTs-DOX has been extended due to the polyethylene glycol coating. Meanwhile, CNTs-DOX is susceptible to acidic conditions while being stable at low pH, which is a desired feature for *in vivo* drug administration.

## 6.2 Proteins and peptides

Protein-based medicines, such as monoclonal antibodies, hormones, cytokines, and therapeutic peptides, have enormous therapeutic promise. However, the physiological instability of protein-based medicines limits their potential applications.<sup>192–194</sup> In other words, whenever nonspecific proteases are administered *in vivo*, proteins can be quickly destroyed prior to reaching their target locations. As a result, competent delivery methods are required to increase protein stability to achieve increased effectiveness. A variety of techniques have been used to improve protein stability and therapeutic effectiveness using carbon nanomaterial-mediated delivery systems *via* noncovalent bonding or covalent conjugation.<sup>195–199</sup> In one study, bovine insulin was physically adsorption-loaded onto NDs, and the ND-insulin complex dissociated pH-dependently under alkaline conditions.<sup>197</sup> *In vitro* tests revealed that the packed insulin was inactive at neutral pH and thus dissolved only in an alkaline medium. Another study looked into NDs' ability to transport antibodies.<sup>200</sup> NDs were found to readily bond with the antibodies and the resulting ND-antibody complex was found to be stable in solution with no antibody releases also after ten days. When acclimated to physiological circumstances, these ND-antibody complexes were prompted to release, but the functioning of Abs was retained during adsorption/desorption processes. CNTs were also utilized to attach to different proteins noncovalently and nonspecifically ( $\approx 80$  kDa). Following cell line uptake, the protein–nanotube conjugates were liberated from the endosomal membrane and entered the cytoplasm to fulfill biological activities.<sup>201</sup>

## 6.3 Gene delivery

A new treatment has gained popularity due to its capacity to actively regulate the expressions of certain proteins that play critical roles in disease development by introducing foreign genetic elements into host cells. However, genetic materials like DNA, plasmid DNA, mRNA, siRNA, and shRNA were unstable in biological systems, posing a significant barrier to further translations. As a consequence, creating vehicles that may improve nucleic acid stability as well as targeted selectivity is a critical factor in paving the road for therapeutic applications. Furthermore, due to the significant potential for immune reaction and carcinogenicity concerns posed by viral vectors, scientists have switched their focus to nonviral vectors, specifically nanocarriers.<sup>202–205</sup> Efficient nucleic acid transport into cells and the release of nucleic acids are required for efficient transfection.<sup>206</sup> Significant efforts have been made to create carbon nanostructures suitable for gene transfer. Notably, NDs and their complexes with propionyl-ethylenimine (PEI) have very low toxicity and excellent biocompatibility, whilst also maintaining high transfection when

trying to deliver plasmid, siRNA, and miRNA typically *via* ionic attraction among both nucleic acid and PEI-modified NDs.<sup>206–209</sup> In one siRNA delivery study, the ND-PEI complex was shown to have higher transfection efficacy under biological circumstances when compared to lipofectamine, the commercial reagent for transfection, indicating the translational promise of this biodegradable siRNA delivery method.<sup>208,210</sup> Similarly, research has been carried out to construct different complexes for gene transfer based on fullerenes.<sup>178,211–214</sup> Maeda-Mamiya *et al.* developed a cationic tetraaminofullerene with high hydrophilicity for plasmid DNA transport.<sup>215</sup> Their findings revealed that delivering the insulin 2 gene increased plasma insulin levels while decreasing blood glucose levels in female C57/BL6 mice. Fullerene derivatives are an excellent therapeutic material for gene transfer. Furthermore, no acute toxicity of the fullerene complex was found following administration. CNTs have also shown their potential as a method for gene transfer. Plasmid DNA was the very first form of nucleic acid effectively transfected *in vitro* by CNTs. Furthermore, CNTs have been used to transfer several types of plasmid DNA since then, such as the green fluorescent protein (GFP) gene.<sup>216–219</sup> Notwithstanding, there has been very little *in vivo* research on plasmid DNA delivered by CNTs. SWCNT-siRNA conjugates with cleavable links were discovered by Kam *et al.* to effectively transport siRNA into cells and downregulate the targeted protein.<sup>220</sup> Following this groundbreaking discovery, an increasing number of studies on CNTs as an excellent platform for siRNA delivery, both *in vitro* and *in vivo*, have been conducted.<sup>221–226</sup> The CNTs were shown to be capable of transfecting difficult cell types such as skeletal muscle cells, primary cellular membranes, and T cells.

## 6.4 Photothermal therapy (PTT)

Fluorescence with emission wavelengths ranging from visible to near-infrared allows certain carbon nanomaterials to be used for both bioimaging and therapy. When photosensitizers concentrate in certain tissues, electromagnetic radiation may be used to heat the tissues, causing photocoagulation and cell death.<sup>227</sup> CNTs with surface modifications can avoid detection by the immune response. Furthermore, CNTs have high absorbance in the near-infrared range, which penetrates deeper into the tissue than the visible range. Carbon nanotubes are an excellent photothermal agent because of these benefits. SWCNTs (single-walled carbon nanotubes) were the first carbon nanomaterials to be developed for photothermal treatment.<sup>228</sup> After CNTs delivered oligonucleotides to cells, a NIR pulsed laser caused endosomal rupture, allowing the loaded oligonucleotides to enter the nucleus. Meanwhile, constant near-infrared radiation caused cell death. In this investigation, SWCNTs served as both a molecular payload and a photosensitizer. SWCNTs can indeed be delivered into the tumour by intratumoral or intravenous injections.<sup>166,229</sup>

## 6.5 Photodynamic therapy (PDT)

A further remarkable photochemical characteristic of fullerene is its photoexcitation capacity. Ground state, singlet C60 may

absorb photons after being stimulated to triplet C60 by photo-excitation. This transfers the stored energy to nearby oxygen molecules, which then converts them into ROS (oxygens and free radicals) through both energy and electron transfer.<sup>178,230–232</sup> Apparently, ROS are very active in DNA breakage and hence have the potential to be cytotoxic. As a result, C60 molecules can be used as photosensitizers in photodynamic treatment.<sup>233</sup> CNTs can be used to transport photosensitizers for PDT, and a few studies have used CNTs themselves as a photosensitizer.<sup>167,171</sup> Shi *et al.* used pep stack interaction to connect hyaluronic acid-modified carbon nanotubes (HA-CNTs) with high water solubility with HMME (PDT agent). The resulting HMME-HA-CNTs, which possessed combined photodynamic and photothermal characteristics, inhibited tumour development including both *in vivo* and *in vitro*.<sup>234,235</sup>

## 6.6. Optical imaging

Because of their remarkable optical characteristics, carbon nanostructures have received a lot of attention in bio-imaging.<sup>158</sup> SWCNTs, for example, exhibit inherent fluorescence properties at different wavelengths (1000–1700 nm), allowing them to be used for deep-tissue fluorescence microscopy due to decreased photon scattering.<sup>236–238</sup> NDs have a relatively extended fluorescence lifetime, making them excellent for differentiating NDs-labeled fluorescence from tissue autofluorescence.<sup>239</sup> Furthermore, due to their inherent photoluminescence, fullerenes (C60) are used in fluorescence imaging.<sup>240–243</sup> This self-fluorescence of NDs is primarily caused by nitrogen impurities and their assimilation into the diamond crystal gap during the manufacturing process.<sup>244,245</sup> Fluorescent nanoparticles, in particular, combine the advantages of quantum dots, biocompatibility, and complex surface chemistry, making them ideal for *in vivo* imaging.<sup>246</sup>

CNTs were employed as molecular transporters in several experiments to transfer organic fluorophores in a cell for fluorescence imaging.<sup>247</sup> Cherukuri *et al.* discovered the intrinsic fluorescence of SWCNTs and photographed their intracellular dispersion in macrophages. This research establishes a novel technique for SWCNTs to be used in bioimaging directly through their inherent fluorescence.<sup>248</sup> SWCNTs are light enough to be observed within mice at high frame rates as useful fluorophores. Based on this, Raman spectroscopy can provide researchers with information about composites. SWCNTs have a Raman peak in the graphitic band that can be distinguished from the background autofluorescence. Because of their high scattering cross-section, SWCNTs could be used as spectroscopic labels and probes in biomedical imaging. Raman spectroscopy was also used to detect SWCNT dispersion in different tissues of mice *ex vivo*, as well as to assess SWCNT circulation *via* intravenous administration. In addition, Raman imaging of CNTs was used *in vivo* in several studies.<sup>249–252</sup> Overall, SWCNTs are recognized as excellent contrast agents for thermoacoustic imaging as well as photothermal imaging.

## 6.7 Non-optical imaging

Carbon nanostructures are excellent light absorbers across the entire visible and near-infrared spectrum, making them ideal for photoacoustics. Meanwhile, because of their low fluorescence quantum outputs, they could more efficiently convert incoming photons to heat. SWCNTs were the first and most widely used photoacoustic imaging nanostructures. Several studies on photoacoustic imaging with SWCNTs *in vivo* have been published.<sup>250,253</sup> One fascinating study combined nanocomposites with photoacoustic responses to Au-coated CNTs with an absorption maximum at distinct wavelengths to generate a two-color photoacoustic image platform. Although tumour cells differ in their own expression, the two-color photoacoustic imaging nanoparticles system proves to be more specific in identifying tumour cells.<sup>254</sup> Overall, SWCNTs are recognized as excellent contrast agents for thermoacoustic imaging as well as photothermal imaging.

## 6.8 Clinical diagnostics

Computerized tomography (CT), magnetic resonance imaging (MRI), and positron emission tomography (PET) are commonly used in clinical diagnostics. MRI is becoming an increasingly common technique for diagnosing due to the unavailability of ionizing radiation.<sup>255</sup> Contrast compounds are commonly used to increase the quality and resolution of MRI. Several contrast compounds include paramagnetic metals, *e.g.*, Fe, Gd, and Mn.<sup>256</sup> Traditional juxtaposition agents, on the other hand, are frequently tiny molecules, and several studies have also shown that Gd-based contrast agents can cause nephrogenic systemic fibrosis (NSF), particularly in people with end-stage renal disease.<sup>257,258</sup> As a consequence, it is critical to create innovative MRI contrast agents with enhanced tissue selectivity and safety. Facet-specific electrostatic force on NDs has played an important role in the coordination of water molecules near to the ND surface, which may be used to produce an ND-metal complex, resulting in enhanced interactions amongst molecules of water and metal ions in behavioral sciences.<sup>177</sup> Hou *et al.*, for example, developed the ND-Mn complex, a dual-mode contrast agent that improved both *T*1 (longitudinal relaxation time) and *T*2 (transverse relaxation time) weighted MRI.<sup>259</sup> These ND-Mn complexes exhibited improved contrast imaging while decreasing the quantity of toxic-free Mn<sup>2+</sup> ions inside the circulatory system, as proved by utilizing an orthotopic liver cancer animal model. Metallofullerene is a potential class of MRI contrast agents.<sup>260,261</sup> The tight network comprising atoms has the benefit of avoiding metal atoms leaking from the fullerene cage whilst preserving all of the metals' physical characteristics.<sup>262</sup> CNTs can potentially be utilized as a distribution platform for contrast agents such as Gd<sup>3+</sup>.<sup>263</sup> CNTs, on the other hand, could be used as MRI agents with the metal contaminants at the ends acting as residual catalysts. SWCNTs were synthesized at high pressure (30–50 atm) using Fe(CO)<sub>5</sub> as the iron-containing catalyst precursor, resulting in iron oxide nanoparticles connected to the ends of the SWCNTs. This pro-

cedure is known as the HiPco technique. Researchers reported the versatility of SWCNTs/iron oxide nanoparticles, which were ingested by macrophage cells and visualized using MRI and near-IR mapping.<sup>264</sup>

### 6.9 Diagnosis and theranostics

Carbon nanostructures are recognized as a cutting-edge biosensing substrate due to their large surface-sensitive area and superior optical and electrical properties.<sup>265</sup> In one study, embedded digital release delivery & sensing devices on ND-peptide complexes were proposed utilizing stimuli-responsive devices.<sup>199</sup> Many of the peptides that could be selectively broken by MMP-9 (matrix metalloproteinase-9) had also been covalently bonded to NDs. MMP-9 is a type of endopeptidase, whose level of expression has been demonstrated to be predictive of cancer spread. Furthermore, the MMP-9-specific solid substrate peptide was fluorescently labeled, allowing MMP-9 protease activity in cleavage of the peptides to be measured and connected to MMP-9 activity. Notably, the formation of ND-peptide complexes protects the peptides from protease cleavage. This quantifiable stimuli-responsive output function, together with improved peptide stability, provides compelling evidence for the development of carbon nanostructures-mediated biosensors for metastasis diagnosis.

Theranostics refers to a significant strategy that combines therapeutic functionality with imaging in a single device. Carbon nanomaterials-based electrochemical biosensors provide a unique class of biosensors, with enhanced conductivity and readily investigated surface region.<sup>266</sup> Petrakova *et al.* created a fluorescence ND-based system for nucleic acid transport and label-free intracellular tracking.<sup>206</sup> The sensing functionality was accomplished by using nitrogen-vacancy colour centers, which offer persistent nonblinking luminosity. The molecular procedures of binding and releasing DNA from fluorescent ND surfaces will cause a change in the electrical charge, allowing nucleic acid transfection and payload release inside of cells to be observed. This inventive device concurrently innovates techniques for nucleic acid transport and imaging while avoiding interference with cellular nucleic acid processes.

CNTs were employed in the construction of enzyme biosensing due to their high aspect ratio, which aids in biomolecular conjugation. Glucose sensing is a significant application of currently utilized biosensors. Under aerobic circumstances, SWCNTs FET biosensors may monitor glucose by catalyzing glucose to gluconic acids and hydrogen peroxide.<sup>267</sup> DNA biosensors are another type of CNT biosensor that is frequently utilized. The CNT-DNA complex has been created to target various molecules based on the fact that single-strand DNA (ssDNA) can securely attach to CNTs but double-strand DNA (dsDNA) cannot, but SWCNTs, in general, function as transducers in sensors, translating and amplifying DNA hybridised on Au into an electrical signal. It was stated that SWCNT-FET DNA sensors may be readily linked with large multiple sensors for microscopy.<sup>268</sup> SWCNT DNA sensing is less difficult to develop than optical or other electrochemical techniques.

### 6.10 Tissue engineering and repair

Carbon nanotubes' shape and structure lend themselves particularly well to applications in stem cell therapy, potentially leading to stem cell growth and banking.<sup>177</sup> Different cells in the brain have been reported to grow effectively on the scaffolds of CNTs. Chemically processed SWCNTs with negative charge were capable of attracting calcium cations, resulting in nucleation and the beginning of the crystallization of hydroxyapatite (HA) as a scaffold for the development of artificial bone material.<sup>269</sup> The advancement direction of HA can be controlled using various bifunctional SWCNTs. MWCNTs-coated nanowires have been shown to improve neurite advancement of rat dorsal root ganglia (DRG) neurons as well as tight junction kinase (FAK) expression in PC-12 (pheochromocytoma) cells through neural tissue engineering.<sup>270</sup> Another usage of CNT scaffolds is in heart tissue development. CNT-incorporated photocross-linkable gel methacrylate (GelMA) demonstrated excellent rigidity and electrophysiological capabilities while lowering electrical resistance, showing potential as cardiac scaffolding.<sup>271</sup>

A polypyrrole (Ppy) array has also been used to regulate stem cell activities with CNTs.<sup>272</sup> The Ppy array, which provided both dynamic attachment and detachment stimuli on cell surfaces, may transition from highly adhesive hydrophobic CNTs to less sticky hydrophilic nanotips *via* an electrochemical oxidation process. NDs, in addition to CNTs, have been created as nanocomposite hydrogels for tissue engineering, especially stem cell-guided regeneration.<sup>273,274</sup> As a 3D scaffold, a hydrogel was produced utilizing photocross-linkable GelMA and NDs. The addition of NDs improved network stiffness, and therefore increased the turning force produced by human adipose cell lines. Interestingly, NDs are also used in root canal therapy (RCT), which is currently being studied in medical tests.<sup>177,275,276</sup>

In one investigation, NDs were implanted with gutta-percha, a benign thermoplastic polymer composed of gutta-percha latex, zinc oxide, a radio pacifier to allow for X-ray imaging to monitor therapy progress, and a plasticizer.<sup>275,277</sup> Namely, using thermoplastics for RCT obturation to prevent reinfection and bone loss after RCT was the current standard. Sustained apical wound healing was documented during interventional therapy, with no reinfection or discomfort issues.

## 7. Emerging high-entropy alloy NPs

High-entropy alloys (HEAs) are a new category of potential electrocatalysts that have recently been identified. HEAs are single solid solutions made up of 5 or more constituents in roughly equal amounts, helping to bring together previously inaccessible element combinations as binary or ternary metals thus according with Hume-Rothery Rules.<sup>278–280</sup> The multi-element characteristic of these alloys results in high mixing entropy, which allows for the development of solid solutions in simplified crystal structures.<sup>281</sup> These characteristics imply that their

textural complexity may provide a unique set of improved microstructure and properties.<sup>282</sup> Furthermore, the low atomic diffusivity that results from the high configuration entropy may also provide excellent strength in corrosive catalytic surroundings.<sup>283</sup> These properties open up a plethora of possibilities for HEA-based catalyst design. Recent studies show that HEA NPs with lower Pt content can have mass activities that are significantly higher than Pt or C for both oxygen reduction (ORR) and durability.<sup>284,285</sup> Fabrication approaches for HEAs, on the other hand, in NP forms with large surface areas are needed. Previously, HEAs were created using thermal techniques wherein the metal ingots were rapidly chillcast to form bulk materials.<sup>286</sup> Jin and colleagues recently created nanoporous HEA AlNiCoIrMo first before melting the ingredients together, followed by chemically dealloying in alkaline medium.<sup>287</sup> Furthermore, HEAs were synthesised as size-controlled NPs using a carbothermal shock technique, in which flash heating and cooling of metals in the presence of an NP support was critical to their creation.<sup>288</sup> The majority of colloidal routes to metallic NPs rely on metal salt reducing, which occurs at different rates in the case of HEAs primed with five or more metal precursors. Synthetically, downsizing HEAs to the nanoscale level has been difficult because most colloidal pathways to metal NPs depend heavily on metal salt reducing,

which takes place at varying rates.<sup>289</sup> Bondesgaard and colleagues described a colloidal method for producing HEA nanocatalysts in an innovative solvothermal environment wherein metal acetylacetone precursors were deeply involved in a  $\text{CH}_3\text{COCH}_3 + \text{C}_2\text{H}_5\text{OH}$  mixture to monitor redox reactions.<sup>290</sup> Xia and colleagues investigated the heat transfer stability of shape-tuned core-shell Pd@PtNPs using *in vivo* electron microscopy. The results showed alloying of core and shell at elevated temperatures where increased heat capacity promotes the nanocrystal formation.<sup>291</sup> Yang *et al.* discovered that deoxidation and metal segregation can transform core-shell Ni@Co NPs into alloy NiCo NPs at 600 °C.<sup>292</sup> A universal colloid approach for HEA NPs is still needed, but it might open up new possibilities in catalysts and well beyond.

Recently, Chen *et al.* developed a controlled approach for HEA NP synthesis based mostly on the colloidal processing of core@shell NPs as compared to sole HEA NPs.<sup>293</sup> The authors used a seed-mediated co-reduction method to create core-shell PdCuB2@PtNiCo NPs, which would then be annealed at extreme temperatures to promote transport, mixing, as well as the formation of HEA NPs. Fig. 13 depicts the process diagram again for the synthesis of HEA NPs. The average size of the HEA NPs was 10.4–0.4 nm (Fig. 13a and b). The compositional analysis revealed the presence of Pd, Cu, Pt, Ni, and Co in

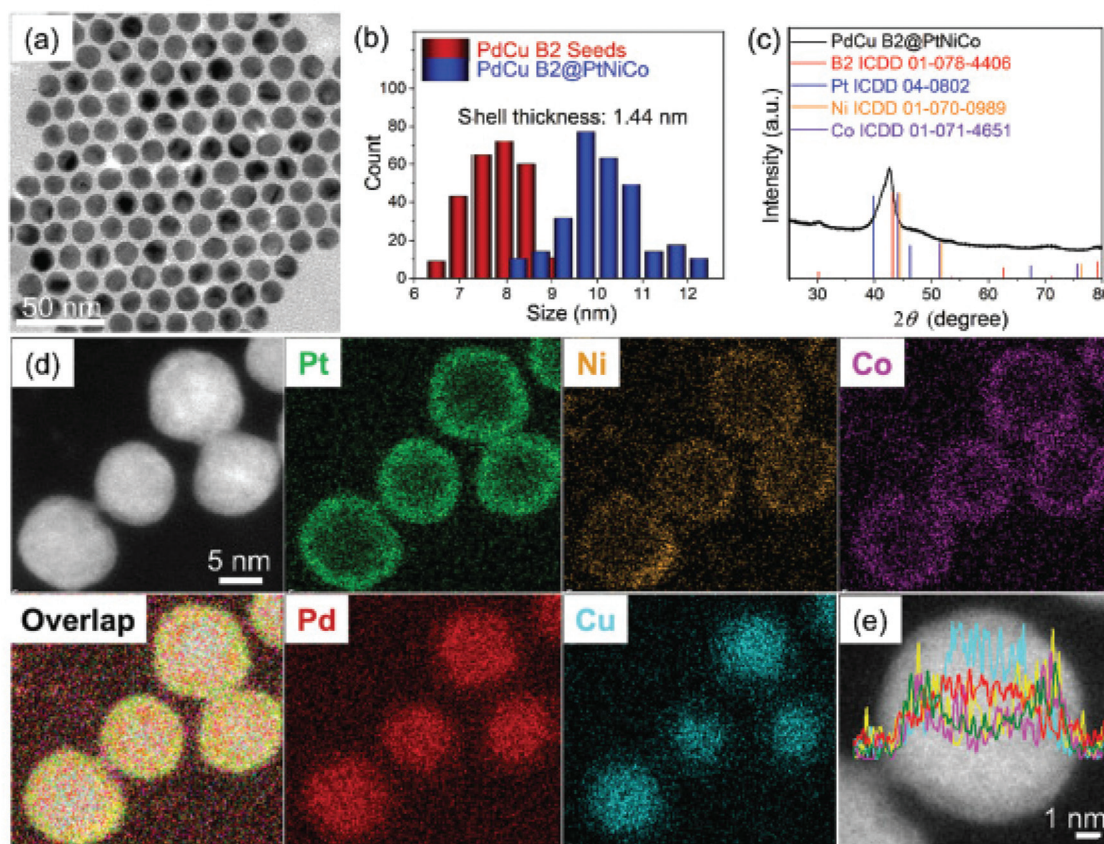


**Fig. 13** (a) Morphology and composition analysis of PdCu B2@PtNiCo NPs. (a) TEM image, (b) particle size distribution, (c) phase analysis, (d and e) area and line mapping reproduced from ref. 293 with permission from [Royal Society of Chemistry], copyright [2021].

atomic fractions of 20%, 17%, 22%, 21%, and 20%, respectively. The phase evolution revealed the presence of PdCu B2 phase and a face-centered solid solution structure (Fig. 13c). Pd and Cu were found to be localised inside the core, whereas Pt, Ni, and Co were found to be distributed on the shell (Fig. 13d and e). However, this is only the tip of the iceberg in terms of HEAs, as many experimental studies are being carried out in the near future to investigate the implementations of these HEA NPs for a wide range of applications.

## 8. Effects of nanomaterials on living systems

The rapid advances in nanomaterials have raised concerns about the potential risks associated with their use and effective utilization on human health and the environment. Obviously, nanoparticles are more active than their bulk counterpart, which may necessitate further research before they are applied to humans. Nanoparticles have been studied in various living models, including cell models, mouse models, and human models. According to earlier investigation, excessive exposure can lead to accumulation in the organs. For example, Mats Hulander *et al.*<sup>294</sup> reported that noble metals can be used as biomaterials due to their antimicrobial and anti-allergic properties. The utilization of metals, such as silver colloidal NPs, significantly raises the risk of night blindness, shoulder pain, lung and neurological diseases. In addition, a few other skin allergies have been reported in association with using colloidal metal nanoparticles.<sup>295</sup> In the case of plants, NPs combat pathological infections and are used as growth adjuvants and nutrient ingredients.<sup>296,297</sup> NPs can be associated with agrochemicals and other substances to deliver or regulate chemicals in plant cell walls, cells, lipid peroxidation, and DNA damage.<sup>298,299</sup> There are many studies that show NP toxicity to microbes, plants, and animals.<sup>298,300</sup> Zhu *et al.*<sup>301</sup> observed that noble metals have been used as a multi-functional cancer therapy due to their exceptional surface plasmon responses. Furthermore, as a consequence of rapid development of pharmaceutical industries, many hazardous pollutants are produced as byproducts. Conventional biological treatment presents a significant challenge in decomposing these NPs. Due to their excellent absorption and dissociating ability, metallic NPs easily solve such problems. In this way, nanoparticles not only benefit human life but also help to reduce pollution in the environment.

## 9. Conclusions and future remarks

Since prehistoric days, noble metal NPs and carbon nanostructures have been found in a variety of purposes ranging from colouring glass to treating complex mental illnesses. Colloidal Au has a long history of usage in medicinal applications. Ag NPs have indeed been used as antibacterial agents in biomedicine. Metal NPs show significant scattering and

absorption of electromagnetic irradiation at the LSPR spectrum, making them more suitable for biomedical activities. MNPs have shown their potential in various bioimaging techniques for tumor identification and drug delivery to cells. Due to the advancement of nanoscience and nanotechnology, carbon nanostructures have boosted biomedicine and healthcare. The optical characteristics of carbon nanostructures are strongly dependent on particulate shape and size for various medical diagnostic tools such as MRI, CT, and PET. Nanostructure patterns including nanoprisms, nanotubes, and nano core-shells have all been used successfully in bioengineering applications.

Numerous different functionalization approaches were used to improve nanostructure dispersibility and biocompatibility in physiological, image analysis, tissue engineering and repair, and drug delivery areas. GNPs were also utilised in Ayurvedic medicine as bhasma. Due to their excellent photothermal characteristics, graphene, CNTs, and NDs nanostructures have been used in theranostic applications. As a consequence, the side effects of chemotherapy could be avoided. Multiple research findings on bio-applications of metal and carbon nanostructures are available in the literature, but there are many limitations in this research and so many new possibilities. In spite of these developments, certain obstacles to the widespread usage of nanomaterials in biomedicine still exist. Due to a wide distribution of sizes, a poor signal-to-noise (S/N) ratio may be present in imaging. This can be solved by choosing an optimum size and shape for each application in biomedicine. The NPs' size reduction might improve their applicability chances in larger biomedical fields. Functionalization of NPs benefits their attachment to the physiological setting, cell growth and drug delivery. In addition, greater cost and experimentation techniques hinder market access. Overall, NPs, when used with greater care and optimization, can be an attractive alternative for advanced biological applications because of their ability to control nanoscale structure, morphology, synthesis process, and price.

## Author contributions

NK: Conceptualization, investigation, methodology; PC: formal analysis and investigation; MM: methodology and data curation; MKM: methodology; NK and AS: writing – original draft; AS: project administration; AS: writing – review and editing.

## Conflicts of interest

The authors declare no conflicts of interest.

## References

- 1 D. Huo, M. J. Kim, Z. Lyu, Y. Shi, B. J. Wiley and Y. Xia, One-Dimensional Metal Nanostructures: From Colloidal

Syntheses to Applications, *Chem. Rev.*, 2019, **119**, 8972–9073.

- 2 J. L. West and N. J. Halas, Engineered Nanomaterials for Biophotonics Applications: Improving Sensing, Imaging, and Therapeutics, *Annu. Rev. Biomed. Eng.*, 2003, **5**, 285–292.
- 3 R. Paull, J. Wolfe, P. Hébert and M. Sinkula, Investing in nanotechnology, *Nat. Biotechnol.*, 2003, **21**, 1144–1147.
- 4 N. Chen, Y. Zhang, H. Liu, X. Wu, Y. Li, L. Miao, Z. Shen and A. Wu, High-Performance Colorimetric Detection of  $Hg^{2+}$  Based on Triangular Silver Nanoprisms, *ACS Sens.*, 2016, **5**, 521–527.
- 5 E. C. Dreaden, A. M. Alkilany, X. Huang, C. J. Murphy and M. A. El-Sayed, The golden age: Gold NPs for biomedicine, *Chem. Soc. Rev.*, 2012, **41**, 2740–2779.
- 6 K. Sztabnera, M. Gorzkiewicz and B. Klajnert-Maculewicz, Gold NPs in Cancer Treatment, *Mol. Pharm.*, 2019, **16**, 1–23.
- 7 L. Jia, Global Governmental Investment in Nanotechnologies, *Curr. Nanosci.*, 2005, **1**, 263–266.
- 8 Y. Xia, W. Li, C. M. Cobley, J. Chen, X. Xia, Q. Zhang, M. Yang, E. C. Cho and P. K. Brown, Gold Nanocages: From Synthesis to Theranostic Applications, *Acc. Chem. Res.*, 2011, **44**, 914–924.
- 9 W. Zhu, J. Zhao, Q. Chen and Z. Liu, Nanoscale metal-organic frameworks and coordination polymers as theranostic platforms for cancer treatment, *Coord. Chem. Rev.*, 2019, **398**, 113009–113023.
- 10 Y. Liu, L. Yang and Y. Shen, Hydrothermal Synthesis of Gold Nanoplates and their Structure-Dependent LSPR Properties, *J. Mater. Res.*, 2018, **33**, 2671–2679.
- 11 J. Alexander, History of the Medical Use of Silver, *Surg. Infect.*, 2009, **10**, 289–292.
- 12 L. A. Dykman and N. G. Khlebtsov, Gold NPs in Biology and Medicine: Recent Advances and Prospects, *Acta Nat.*, 2011, **3**, 34–55.
- 13 A. Gautam, P. Komal, P. Gautam, A. Sharma, N. Kumar and J. P. Jung, Recent Trends in Noble Metal Nanoparticles for Colorimetric Chemical Sensing and Micro-Electronic Packaging Applications, *Metals*, 2021, **11**, 329.
- 14 Y. Chen, Z. Fan, Z. Zhang, W. Niu, C. Li, N. Yang, B. Chen and H. Zhang, Two-Dimensional Metal Nanomaterials: Synthesis, Properties, and Applications, *Chem. Rev.*, 2018, **118**, 6409–6455.
- 15 X. Wei, X. Wang, B. Gao, W. Zou and L. Dong, Facile Ball-Milling Synthesis of CuO/Biochar Nanocomposites for Efficient Removal of Reactive Red 120, *ACS Omega*, 2020, **5**, 5748–5755.
- 16 I. Korczagin, S. Golze, M. A. Hempenius and G. J. Vancso, Surface Micropatterning and Lithography with Poly(Ferrocenylmethylphenylsilane), *Chem. Mater.*, 2003, **15**, 3663–3668.
- 17 S. H. Kim, B. Y. H. Liu and M. R. Zachariah, Synthesis of Nanoporous Metal Oxide Particles by a New Inorganic Matrix Spray Pyrolysis Method, *Chem. Mater.*, 2002, **14**, 2889–2899.
- 18 A. S. Susha, M. Ringler, A. Ohlinger, M. Paderi, N. LiPira, G. Carotenuto, A. L. Rogach and J. Feldmann, Strongly Luminescent Films Fabricated by Thermolysis of Gold-Thiolate Complexes in a Polymer Matrix, *Chem. Mater.*, 2008, **20**, 6169–6175.
- 19 C. Suryanarayana, Mechanical milling and alloying, *Prof. Mater. Sci.*, 2001, **46**(1–2), 1–184.
- 20 M. Faris and M. Suhaib, Introduction to Powder Metallurgy: A Review, *IARJ. Eng. Technol.*, 2021, **2**(3), 1–7.
- 21 M. Zhu, G. Baffou, N. Meyerbröker and J. Polleux, Micropatterning Thermoplasmonic Gold Nanoarrays To Manipulate Cell Adhesion, *ACS Nano*, 2012, **6**, 7227–7233.
- 22 J. Marques-Hueso, J. A. S. Morton, X. Wang, E. Bertran-Serra and M. P. Y. Desmulliez, Photolithographic Nanoseeding Method for Selective Synthesis of Metal-Catalysed Nanostructures, *Nanotechnology*, 2019, **30**, 15302–15309.
- 23 D. Qin, Y. Xia and G. M. Whitesides, Soft lithography for Micro- and Nanoscale Patterning, *Nat. Protoc.*, 2010, **5**, 491–502.
- 24 S. V. Sreenivasan, Nanoimprint Lithography Steppers for Volume Fabrication of Leading-Edge Semiconductor Integrated Circuits, *Microsyst. Nanoeng.*, 2017, **3**, 17075–17093.
- 25 J. C. Garno, Y. Yang, N. A. Amro, S. Cruchon-Dupeyrat, S. Chen and G.-Y. Liu, Precise Positioning of NPs on Surfaces Using Scanning Probe Lithography, *Nano Lett.*, 2003, **3**, 389–395.
- 26 A. Heuer-Jungemann, N. Feliu, I. Bakaimi, M. Hamaly, A. Alkilany, I. Chakraborty, A. Masood, M. F. Casula, A. Kostopoulou, E. Oh, *et al.*, The Role of Ligands in the Chemical Synthesis and Applications of Inorganic NPs, *Chem. Rev.*, 2019, **119**, 4819–4880.
- 27 A. Gautam, S. Mukherjee and S. Ram, Controlled Novel Route to Synthesis and Characterization of Silver Nanorods, *J. Nanosci. Nanotechnol.*, 2010, **10**, 4329–4334.
- 28 A. Gautam, G. P. Singh and S. Ram, A Simple Polyol Synthesis of Silver Metal Nanopowder of Uniform Particles, *Synth. Met.*, 2007, **157**, 5–10.
- 29 D. D. Evanoff and G. Chumanov, Size-Controlled Synthesis of NPs. 1. “Silver-Only” Aqueous Suspensions via Hydrogen Reduction, *J. Phys. Chem. B*, 2004, **108**, 13948–13956.
- 30 V. V. Tatarchuk, A. P. Sergievskaya, T. M. Korda, I. A. Druzhinina and V. I. Zaikovsky, Kinetic Factors in the Synthesis of Silver NPs by Reduction of  $Ag^+$  with Hydrazine in Reverse Micelles of Triton N-42, *Chem. Mater.*, 2013, **25**, 3570–3579.
- 31 S. Fountoulaki, V. Daikopoulou, P. L. Gkizis, I. Tamiolakis, G. S. Armatas and I. N. Lykakis, Mechanistic Studies of the Reduction of Nitroarenes by  $NaBH_4$  or Hydrosilanes Catalyzed by Supported Gold NPs, *ACS Catal.*, 2014, **4**, 3504–3511.
- 32 S. Ahmad, S. Munir, N. Zeb, A. Ullah, B. Khan, J. Ali, M. Bilal, M. Omer, M. Alamzeb, S. M. Salman, *et al.*, Green Nanotechnology: A Review on Green Synthesis of Silver NPs An Ecofriendly Approach, *Int. J. Nanomed.*, 2019, **14**, 5087–5107.

33 A. Gautam, P. Tripathy and S. Ram, Microstructure, topology and X-ray diffraction in Ag-Metal Reinforced Polymer of Polyvinyl Alcohol of Thin Laminates, *J. Mater. Sci.*, 2006, **41**, 3007–3016.

34 J. H. Schulman, W. Stoeckenius and L. M. Prince, Mechanism of Formation and Structure of Micro Emulsions by Electron Microscopy, *J. Phys. Chem.*, 1959, **63**, 1677–1680.

35 R. K. Sandeep, B. Lies, H. Lyu and H. Qin, Laser Ablation of Polymers: A Review, *Procedia Manuf.*, 2019, **34**, 316–327.

36 N. Dahal, S. García, J. Zhou and S. M. Humphrey, Beneficial Effects of Microwave-Assisted Heating versus Conventional Heating in Noble Metal Nanoparticle Synthesis, *ACS Nano*, 2012, **6**, 9433–9446.

37 E. Guo, Z. Zeng, X. Shi, X. Long and X. Wang, Electrical Transport Properties of Au Nanoparticles and Thin Films on Ge Probed Using a Conducting Atomic Force Microscope, *Langmuir*, 2016, **32**(41), 10589–10596.

38 T. Zheng, W. C. H. Choy and Y. Sun, Hybrid Nanoparticle/ Organic Devices with Strong Resonant Tunneling Behaviors, *Adv. Funct. Mater.*, 2009, **19**(16), 2648–2653.

39 A. Pfenning, F. Hartmann, M. R. S. Dias, L. K. Castelano, C. Süssmeier, F. Langer, S. Höfling, M. Kamp, G. E. Marques, L. Worschech and V. L. Richard, Nanothermometer Based on Resonant Tunneling Diodes: From Cryogenic to Room Temperatures, *ACS Nano*, 2015, **9**(6), 6271–6277.

40 B. Sharma, J. S. Kim and A. Sharma, Transparent AgNW-CoNPs conducting film for heat sensor, *Microelectron. Eng.*, 2019, **205**, 37–43.

41 B. Sharma, J. S. Kim and A. Sharma, AgNWs-graphene transparent conductor for heat and sensing application, *Mater. Res. Express*, 2019, **6**, 066312.

42 A. Sharma, S. Das and K. Das, Pulse Electroplating of Ultrafine Grained Tin Coating, in *Electroplating of Nanostructures*, ed. M. Aliofkhazraei, IntechOpen, 2015, DOI: 10.5772/61255. Available from: <https://www.intechopen.com/chapters/49372>.

43 A. Sharma, S. Das and K. Das, Pulse Electrodeposition of Lead-Free Tin-Based Composites for Microelectronic Packaging, in *Electrodeposition of Composite Materials*, ed. A. M. A. Mohamed and T. D. Golden, IntechOpen, 2016, DOI: 10.5772/62036. Available from: <https://www.intechopen.com/chapters/49897>.

44 M. B. Gawande, A. Goswami, F.-X. Felpin, T. Asefa, X. Huang, R. Silva, X. Zou, R. Zboril and R. S. Varma, Cu and Cu-Based Nanoparticles: Synthesis and Applications in Catalysis, *Chem. Rev.*, 2016, **116**(6), 3722–3811.

45 A. Balanta, C. Godard and C. Claver, Pdnanoparticles for C–C coupling reactions, *Chem. Soc. Rev.*, 2011, **40**, 4973–4985.

46 C. Wu, L. Zhou, Y. Zhou, C. Zhou, S. Xia and B. E. Rittmann, Dechlorination of 2,4-dichlorophenol in a hydrogen-based membrane palladium-film reactor: Performance, mechanisms, and model development, *Water Res.*, 2021, **188**, 116465.

47 I. Khan, K. Saeed and I. Khan, Nanoparticles: Properties, applications and toxicities, *Arabian J. Chem.*, 2019, **12**(7), 908–931.

48 J. Park, J. Joo, S. G. Kwon, Y. Jang and T. Hyeon, Synthesis of Monodisperse Spherical Nanocrystals, *Angew. Chem., Int. Ed.*, 2007, **46**, 4630–4660.

49 M. Faraday, The bakerian lecture: Experimental relations of gold (and other metals) to light, *Philos. Trans. R. Soc. London*, 1857, **147**, 145–181.

50 J. Niu, T. Zhu and Z. Liu, One-step seed-mediated growth of 30–150 nm quasi-spherical gold nanoparticles with 2-mercaptosuccinic acid as a new reducing agent, *Nanotechnology*, 2007, **18**, 325607.

51 K. Jiang, D. A. Smith and A. Pinchuk, Size-Dependent Photothermal Conversion Efficiencies of Plasmonically Heated Gold Nanoparticles, *J. Phys. Chem. C*, 2013, **117**(51), 27073–27080.

52 S. Yang, L. Zhou, Y. Sua, R. Zhang and C.-M. Dong, One-pot photoreduction to prepare NIR-absorbing plasmonic gold nanoparticles tethered by amphiphilic polypeptide copolymer for synergistic photothermal-chemotherapy, *Chin. Chem. Lett.*, 2019, **30**(1), 187–191.

53 Y. Yang, Y. Lin, D. Di, X. Zhang, D. Wang, Q. Zhao and S. Wang, Gold nanoparticle-gated mesoporous silica as redox-triggered drug delivery for chemo-photothermal synergistic therapy, *J. Colloid Interface Sci.*, 2017, **508**, 323–331.

54 E. Hwang and H. S. Jung, Organelle-targeted photothermal agents for cancer therapy, *Chem. Commun.*, 2021, **57**, 7731–7742.

55 L. Pan, J. Liu and J. Shi, Nuclear-Targeting Gold Nanorods for Extremely Low NIR Activated Photothermal Therapy, *ACS Appl. Mater. Interfaces*, 2017, **9**(19), 15952–15961.

56 M. S. Khan, S. Pandey, M. L. Bhaisare, G. Geda, A. Talib and H.-F. Wu, Graphene oxide@gold nanorods for chemo-photothermal treatment and controlled release of doxorubicin in mice Tumor, *Colloids Surf., B*, 2017, **160**, 543–552.

57 A. Syafiuddin, Salmiati, M. R. Salim, A. B. H. Kueh, T. Hadibarata and H. Nur, A Review of silver nanoparticles: Research trends, global consumption, synthesis, properties, and future Challenges, *J. Clin. Chem. Soc.*, 2017, **64**, 732–756.

58 A. Kumar, P. K. Vemula, P. M. Ajayan and G. John, Silver-nanoparticle-embedded antimicrobial paints based on vegetable oil, *Nat. Mater.*, 2008, **7**, 236–241.

59 A. Desiréddy, B. E. Conn, J. Guo, B. Yoon, R. N. Barnett, B. M. Monahan, K. Kirschbaum, W. P. Griffith, R. L. Whetten, U. Landman, *et al.*, Ultrastable silver nanoparticles, *Nature*, 2013, **501**, 399–402.

60 Y. Sun and Y. Xia, Shape-controlled synthesis of gold and silver nanoparticles, *Science*, 2002, **298**, 2176–2179.

61 H. A. Atwater and A. Polman, Plasmonics for improved photovoltaic devices, *Nat. Mater.*, 2010, **9**, 205–213.

62 B. L. Ouay and F. Stellacci, Antibacterial activity of silver nanoparticles: A surface science insight, *Nano Today*, 2015, **10**, 339–354.

63 D. Chen, X. Qiao, X. Qiu and J. Chen, Synthesis and electrical properties of uniform silver nanoparticles for electronic applications, *J. Mater. Sci.*, 2009, **44**, 1076–1081.

64 Y. Sun, B. Mayers, T. Herricks and Y. Xia, Polyol synthesis of uniform silver nanowires: a plausible growth mechanism and the supporting evidence, *Nano Lett.*, 2003, **3**, 955–960.

65 A. J. Haes and R. P. V. Duyne, A Nanoscale optical biosensor: sensitivity and selectivity of an approach based on the localized surface plasmon resonance spectroscopy of triangular silver nanoparticles, *J. Am. Chem. Soc.*, 2002, **124**, 10596–10604.

66 T. A. Dankovich and D. G. Gray, Bactericidal paper impregnated with silver nanoparticles for point-of-use water treatment, *Environ. Sci. Technol.*, 2011, **45**, 1992–1998.

67 X.-F. Zhang, Z.-G. Liu, W. Shen and S. Gurunathan, Silver nanoparticles: Synthesis, characterization, properties, applications, and therapeutic approaches, *Int. J. Mol. Sci.*, 2016, **17**, 1534.

68 L. Wang, T. Zhang, P. Li, W. Huang, J. Tang, P. Wang, J. Liu, Q. Yuan, R. Bai, B. Li, *et al.*, Use of synchrotron radiation-analytical techniques to reveal chemical origin of silver-nanoparticle cytotoxicity, *ACS Nano*, 2015, **9**, 6532–6547.

69 K. M. M. A. El-Nour, A. Eftaiha, A. Al-Warthan and R. A. A. Ammar, Synthesis and applications of silver nanoparticles, *Arabian J. Chem.*, 2010, **3**, 135–140.

70 J. Park, S.-H. Cha, S. Cho and Y. Park, Green synthesis of gold and silver nanoparticles using gallic acid: Catalytic activity and conversion yield toward the 4-nitrophenol reduction reaction, *J. Nanopart. Res.*, 2016, **18**, 166.

71 K.-S. Lee and M. A. El-Sayed, Dependence of the enhanced optical scattering efficiency relative to that of absorption for gold metal nanorods on aspect ratio, size, end-cap shape, and medium refractive index, *J. Phys. Chem. B*, 2005, **109**, 20331–20338.

72 D. Aherne, D. M. Ledwith, M. Gara and J. M. Kelly, Optical properties and growth aspects of silver nanoprisms produced by a highly reproducible and rapid synthesis at room temperature, *Adv. Funct. Mater.*, 2008, **18**, 2005–2016.

73 R. Jin, Y. Cao, C. A. Mirkin, K. L. Kelly, G. C. Schatz and J. G. Zheng, Photoinduced conversion of silver nanospheres to nanoprisms, *Science*, 2001, **294**, 1901–1903.

74 S. H. Lee and B.-H. Jun, Silver Nanoparticles: Synthesis and Application for Nanomedicine, *Int. J. Mol. Sci.*, 2019, **20**, 865.

75 S.-H. Kim, H.-S. Lee, D.-S. Ryu, S.-J. Choi and D.-S. Lee, Antibacterial activity of silver-nanoparticles against *Staphylococcus aureus* and *Escherichia coli*, *Korean J. Microbiol. Biotechnol.*, 2011, **39**, 77–85.

76 L. A. Tamayo, P. A. Zapata, N. D. Vejar, M. I. Azócar, M. A. Gulppi, X. Zhou, G. E. Thompson, F. M. Rabagliati and M. A. Páez, Release of silver and copper nanoparticles from polyethylene nanocomposites and their penetration into *Listeria monocytogenes*, *Mater. Sci. Eng.*, 2014, **40**, 24–31.

77 A. Abbaszadegan, Y. Ghahramani, A. Gholami, B. Hemmateenejad, S. Dorostkar, M. Nabavizadeh and H. Sharghi, The effect of charge at the surface of silver nanoparticles on antimicrobial activity against Gram-positive and Gram-negative bacteria: A preliminary study, *J. Nanomater.*, 2015, 720654.

78 T. C. Dakal, A. Kumar, R. S. Majumdar and V. Yadav, Mechanistic basis of antimicrobial actions of silver nanoparticles, *Front. Microbiol.*, 2016, **7**, 1831.

79 C.-Y. Loo, R. Rohanizadeh, P. M. Young, D. Traini, R. Cavaliere, C. B. Whitchurch and W.-H. Lee, Combination of silver nanoparticles and curcumin nanoparticles for enhanced anti-biofilm activities, *J. Agric. Food Chem.*, 2016, **64**, 2513–2522.

80 P. Paril, J. Baar, P. Čermák, P. Rademacher, R. Prucek, M. Sivera and A. Panáček, Antifungal effects of copper and silver nanoparticles against white and brown-rot fungi, *J. Mater. Sci.*, 2017, **52**, 2720–2729.

81 S. Tang and J. Zheng, Antibacterial activity of silver nanoparticles: Structural effects, *Adv. Healthcare Mater.*, 2018, **7**, 1701503.

82 R. H. Kodama, Magnetic nanoparticles, *J. Magn. Magn. Mater.*, 1999, **200**(1), 359–372.

83 A. S. Teja and P. Y. Koh, Synthesis, properties, and applications of magnetic ironoxide nanoparticles, *Prog. Cryst. Growth Charact. Mater.*, 2009, **55**(1), 22–45.

84 L. Mohammed, H. G. Goma, D. Ragab and J. Zhu, Magnetic nanoparticles for environmental and biomedical applications: A review, *Particuology*, 2017, **30**, 1–14.

85 A. K. A. Silva, R. Di Corato, F. Gazeau, T. Pellegrino and C. Wilhelm, Mag-netophoresis at the nanoscale: Tracking the magnetic targeting efficiency ofnanovectors, *Nanomedicine*, 2012, **7**(11), 1713–1727.

86 B. F. Grzeskowiak, Y. Sánchez-Antequera, E. Hammerschmid, M. Döblinger, D. Eber-beck, A. Wózniak, *et al.*, Nanomagnetic activation as a way to controlthe efficacy of nucleic acid delivery, *Pharm. Res.*, 2015, **32**(1), 103–121.

87 E. Tombácz, R. Turcu, V. Socoliu and L. Vékás, Magnetic iron oxide nanoparti-cles: Recent trends in design and synthesis of magnetoresponsivenanosystems, *Biochem. Biophys. Res. Commun.*, 2015, **468**(3), 442–453.

88 R. Mangaiyarkarasi, S. Chinnathambi, S. Karthikeyan, P. Aruna and S. Gane-san, Paclitaxel conjugated  $\text{Fe}_3\text{O}_4@\text{LaF}_3:\text{Ce}^{3+},\text{Tb}^{3+}$  nanoparticles asbifunctional targeting carriers for Cancer theranostics application, *J. Magn. Magn. Mater.*, 2016, **399**, 207–215.

89 J. An, X. Zhang, Q. Guo, Y. Zhao, Z. Wu and C. Li, Glycopolymersmodifiedmagnetic mesoporous silica nanoparticles for MR imaging and targeted drugdelivery, *Colloids Surf. A*, 2015, **482**, 98–108.

90 T. S. Anirudhan, P. L. Divya and J. Nima, Synthesis and characterization ofsilane coated magnetic nanoparticles/glycidylmethacrylate-grafted-maleatedcyclodextrin composite hydrogel as a drug carrier for the controlled deliveryof 5-fluorouracil, *Mater. Sci. Eng., C*, 2015, **55**, 471–481.

91 N. S. Elbialy, M. M. Fathy and W. M. Khalil, Doxorubicin loaded magneticgold nanoparticles for in vivo targeted drug delivery, *Int. J. Pharm.*, 2015, **490**(1–2), 190–199.

92 C. Nazli, G. S. Demirer, Y. Yar, H. Y. Acar and S. Kizilel, Targeted delivery ofdoxorubicin into tumor cells via MMP-sensitive PEG hydrogel-coated magneticiron oxide nanoparticles (MIONPs), *Colloids Surf., B*, 2014, **122**, 674–683.

93 G. Li, L. Cao, Z. Zhou, Z. Chen, Y. Huang and Y. Zhao, Rapamycin loadedmagnetic Fe<sub>3</sub>O<sub>4</sub>/carboxymethyl-chitosan nanoparticles as tumor-targeted drugdelivery system: Synthesis and in vitro characterization, *Colloids Surf., B*, 2015, **128**, 379–388.

94 Z. Chen, L. Zhang, Y. Song, J. He, L. Wu, C. Zhao, *et al.*, Hierarchical targetedhepatocyte mitochondrial multifunctional chitosan nanoparticles for anticancerdrug delivery, *Biomaterials*, 2015, **52**, 240–250.

95 G. I. Frolov, O. I. Bachina, M. M. Zav'yalova and S. I. Ravochkin, Magneticproperties of nanoparticles of 3d metals, *Tech. Phys.*, 2008, **53**(8), 1059–1064.

96 F. Mohammad and N. A. Yusof, Surface ligand influenced free radical pro-tection of superparamagnetic iron oxide nanoparticles (SPIONs) toward H9c2cardiac cells, *J. Mater. Sci.*, 2014, **49**(18), 6290–6301.

97 A. Singh and S. K. Sahoo, Magnetic nanoparticles: A novel platform for cancertheranostics, *Drug Discovery Today*, 2014, **19**(4), 474–481.

98 P. Periyathambi, W. S. Vedakumari, S. Bojja, S. B. Kumar and T. P. Sastry, Green biosynthesis and characterization of fibrin functionalized iron oxidenanoparticles with MRI sensitivity and increased cellular internalization, *Mater. Chem. Phys.*, 2014, **148**(3), 1212–1220.

99 C. Sanjai, S. Kothan, P. Gonil, S. Saesoo and W. Sajomsang, Chitosan-triphosphate nanoparticles for encapsulation of super-paramagnetic iron oxideas an MRI contrast agent, *Carbohydr. Polym.*, 2014, **104**, 231–237.

100 J. Wang, B. Zhang, L. Wang, M. Wang and F. Gao, One-pot synthesis ofwater-soluble superparamagnetic iron oxide nanoparticles and their MRI contrast effects in the mouse brains, *Mater. Sci. Eng., C*, 2015, **48**, 416–423.

101 S. Xie, B. Zhang, L. Wang, J. Wang, X. Li, G. Yang, *et al.*, Superparamagnetic iron oxide nanoparticles coated with different polymers and their MRI contrast effects in the mouse brains, *Appl. Surf. Sci.*, 2015, **326**, 32–38.

102 J. D. G. Durán, J. L. Arias, V. Gallardo and A. V. Delgado, Magnetic colloids as drug vehicles, *J. Pharm. Sci.*, 2008, **97**(8), 2948–2983.

103 A. H. Castro Neto, F. Guinea and N. M. R. Peres, Drawing conclusions from graphene, *Phys. World*, 2006, **19**, 33.

104 M. Inagaki and F. Kang, Graphene derivatives: graphane, fluorographene, graphene oxide, graphyne and graphdiyne, *J. Mater. Chem. A*, 2014, **2**, 13193–13206.

105 K. S. Novoselov, A. K. Geim, S. V. Morozov, D. Jiang, Y. Zhang, S. V. Dubonos, I. V. Grigorieva and A. A. Firsov, Electric field in atomically thin carbon films, *Science*, 2004, **306**, 666–669.

106 P. Chamoli, R. K. Shukla, A. Bezbaruah, K. K. Kar and K. K. Raina, *Appl. Surf. Sci.*, 2021, **555**, 149663.

107 A. K. Geim, Graphene: status and prospects, *Science*, 2009, **324**, 1530–1534.

108 K. S. Novoselov, D. Jiang, F. Schedin, T. J. Booth, V. V. Khotkevich, S. V. Morozov and A. K. Geim, Two dimensional atomic crystals, *Proc. Natl. Acad. Sci. U. S. A.*, 2005, **102**(30), 10451–10453.

109 C. N. R. Rao, K. Biswas, K. S. Subrahmanyam and A. Govindaraj, Graphene, the new nanocarbon, *J. Mater. Chem.*, 2009, **19**, 2457–2469.

110 K. I. Bolotin, K. J. Sikes, Z. Jiang, M. Klima, G. Fudenberg, J. Hone, P. Kim and H. L. Stormer, Ultrahigh electron mobility in suspended graphene, *Solid State Commun.*, 2008, **146**, 351–355.

111 X. Du, I. Skachko, A. Barker and E. Y. Andrei, Approaching ballistic transport in suspended graphene, *Nat. Nanotechnol.*, 2008, **3**, 491–495.

112 Y. Zhang, Y.-W. Tan, H. L. Stormer and P. Kim, Experimental observation of the quantum Hall effect and Berry's phase in graphene, *Nature*, 2005, **438**, 201–204.

113 W. Choi, I. Lahiri, R. Seelaboyina and Y. S. Kang, Synthesis of graphene and its applications: a review, *Crit. Rev. Solid State Mater. Sci.*, 2010, **35**, 52–71.

114 S. J. Guo and S. J. Dong, Graphene nanosheet: synthesis, molecular engineering, thin film, hybrids, and energy and analytical applications, *Chem. Soc. Rev.*, 2011, **40**, 2644–2672.

115 K. S. Novoselov, Beyond the wonder material, *Phys. World*, 2009, **22**, 27–30.

116 V. Georgakilas, M. Otyepka, A. B. Bourlinos, V. Chandra, N. Kim, K. C. Kemp, P. Hobza, R. Zboril and K. S. Kim, Functionalization of graphene: covalent and noncovalent approaches, derivatives and applications, *Chem. Rev.*, 2012, **112**, 6156–6214.

117 V. Georgakilas, J. N. Tiwari, K. C. Kemp, J. A. Perman, A. B. Bourlinos, K. S. Kim and R. Zboril, Noncovalent functionalization of graphene and graphene oxide for energy materials, biosensing, catalytic, and biomedical applications, *Chem. Rev.*, 2016, **116**, 5464–5519.

118 T. Kuila, S. Bose, A. K. Mishra, P. Khanra and J. H. Lee, Chemical functionalization of graphene and its applications, *Prog. Mater. Sci.*, 2012, **57**, 1061–1105.

119 Y. Shao, J. Wang, H. Wu, J. Liu, I. A. Aksay and Y. Lin, Graphene based electrochemical sensors and biosensors: a review, *Electroanalysis*, 2010, **22**, 1027.

120 O. Akhavan, E. Ghaderi and R. Rahighi, Toward single-DNA electrochemical biosensing by graphene nanowalls, *ACS Nano*, 2012, **6**, 2904–2916.

121 N. Mohanty and V. Berry, Graphene-based singlebacterium resolution biodevice and DNA transistor: interfacing graphene derivatives with nanoscale and microscale biocomponents, *Nano Lett.*, 2008, **8**, 4469–4476.

122 W. Hu, C. Peng, W. Luo, M. Lv, X. Li, D. Li, Q. Huang and C. Fan, Graphene-based antibacterial paper, *ACS Nano*, 2010, **4**, 4317–4323.

123 J. Ma, J. Zhang, Z. Xiong, Y. Yong and X. S. Zhao, Preparation, characterization and antibacterial properties of silver-modified graphene oxide, *J. Mater. Chem.*, 2011, **21**, 3350–3352.

124 K. Yang, J. Wan, S. Zhang, B. Tian, Y. Zhang and Z. Liu, The influence of surface chemistry and size of nanoscale graphene oxide on photothermal therapy of cancer using ultra-low laser power, *Biomaterials*, 2012, **33**, 2206–2214.

125 W. Zhang, Z. Guo, D. Huang, Z. Liu, X. Guo and H. Zhong, Synergistic effect of chemo-photothermal therapy using PEGylated graphene oxide, *Biomaterials*, 2011, **32**, 8555–8561.

126 Z. Liu, J. T. Robinson, X. Sun and H. Dai, PEGylated nanographene oxide for delivery of water-insoluble cancer drugs, *J. Am. Chem. Soc.*, 2008, **130**(33), 10876–10877.

127 C. Heo, J. Yoo, S. Lee, A. Jo, S. Jung, H. Yoo, Y. H. Lee and M. Suh, The control of neural cell-to-cell interactions through non-contact electrical field stimulation using graphene electrodes, *Biomaterials*, 2011, **32**, 19–27.

128 S. Agarwal, X. Zhou, F. Ye, Q. He, G. C. K. Chen, J. Soo, F. Boey, H. Zhang and P. Chen, Interfacing live cells with nanocarbon substrates, *Langmuir*, 2010, **26**, 2244–2247.

129 Y. Chen, H. Vedala, G. P. Kotchey, A. Audfray, S. Cecioni, A. Imberty, S. Vidal and A. Star, Electronic detection of lectins using carbohydrate-functionalized nanostructures: graphene versus carbon nanotubes, *ACS Nano*, 2012, **6**, 760–770.

130 S. Park, *et al.*, Biocompatible, robust freestanding paper composed of a TWEEN/graphene composite, *Adv. Mater.*, 2012, **22**, 1736–1740.

131 H. Y. Mao, S. Laurent, W. Chen, O. Akhavan, M. Imani, A. A. Ashkarran and M. Mahmoudi, Graphene: promises, facts, opportunities, and challenges in nanomedicine, *Chem. Rev.*, 2013, **113**, 3407–3424.

132 C. Chung, Y. K. Kim, D. Shin, S. R. Ryoo, B. H. Hong and D. H. Min, Biomedical applications of graphene and graphene oxide, *Acc. Chem. Res.*, 2013, **46**, 2211–2224.

133 Y. Wang, Z. Li, J. Wang, J. Li and Y. Lin, Graphene and graphene oxide: biofunctionalization and applications in biotechnology, *Trends Biotechnol.*, 2011, **29**, 205–212.

134 Y. Ohno, K. Maehashi and K. Matsumoto, Label-free biosensors based on aptamer-modified graphene field-effect transistors, *J. Am. Chem. Soc.*, 2010, **132**, 18012–18013.

135 O. S. Kwon, S. J. Park, J. Y. Hong, A. R. Han, J. S. Lee, J. S. Lee, J. H. Oh and J. Jang, Flexible FET-type VEGF aptasensor based on nitrogen-doped graphene converted from conducting polymer, *ACS Nano*, 2012, **6**, 1486–1493.

136 S. Mao, G. Lu, K. Yu, Z. Bo and J. Chen, Specific protein detection using thermally reduced graphene oxide sheet decorated with gold nanoparticle antibody conjugates, *Adv. Mater.*, 2010, **22**, 3521–3526.

137 Z. Tang, H. Wu, J. R. Cort, G. W. Bchko, Y. Zhang, Y. Shao, I. A. Aksay, J. Liu and Y. Lin, Constraint of DNA on functionalized graphene improves its biostability and specificity, *Small*, 2010, **6**, 1205–1209.

138 G. Gollavelli and Y. C. Ling, Multi-functional graphene as an in vitro and in vivo imaging probe, *Biomaterials*, 2012, **33**, 2532–2545.

139 C. Hu, *et al.*, One-step preparation of nitrogen-doped graphene quantum dots from oxidized debris of graphene oxide, *J. Mater. Chem. B*, 2013, **1**, 39–42.

140 W. Chen, Y. Peiwei, Y. Zhang, L. Zhang, Z. Deng and Z. Zhang, Composites of Aminodextran-coated Fe3O4 nanoparticles and graphene oxide for cellular magnetic resonance imaging, *ACS Appl. Mater. Interfaces*, 2011, **3**, 4085–4091.

141 A. Pohlmann, *et al.*, Linking non-invasive parametric MRI with invasive physiological measurements (MR-PHYSIOL): towards a hybrid and integrated approach for investigation of acute kidney injury in rats, *Acta Physiol.*, 2013, **207**, 673–689, DOI: 10.1111/apha.12065.

142 H. Hong, *et al.*, In vivo targeting and imaging of tumor vasculature with radiolabeled, antibody-conjugated nanographene, *ACS Nano*, 2012, **6**, 2361–2370.

143 M. Du, T. Yang and K. Jiao, Immobilization-free direct electrochemical detection for DNA specific sequences based on electrochemically converted gold nanoparticles/graphene composite film, *J. Mater. Chem.*, 2010, **20**, 9253–9260.

144 Y. Wang, Y. Shao, D. W. Matson, J. Li and Y. Lin, Nitrogen-doped graphene and its application in electrochemical biosensing, *ACS Nano*, 2010, **4**, 1790–1798.

145 X. Shi, W. Gu, W. Peng, B. Li, N. Chen, K. Zhao and Y. Xian, Sensitive Pb2þ probe based on the fluorescence quenching by graphene oxide and enhancement of the leaching of gold nanoparticles, *ACS Appl. Mater. Interfaces*, 2014, **6**, 25682575.

146 P. K. Ang, A. Li, M. Jaiswal, Y. Wang, H. W. Hou, L. Thong, C. T. Lim and K. P. Loh, Flow sensing of single cell by graphene transistor in a microfluidic channel, *Nano Lett.*, 2011, **11**, 5240–5246.

147 N. Narita, S. Nagagi, S. Suzuki and K. Nakao, Optimized geometries and electronic structures of graphyne and its family, *Phys. Rev. B: Condens. Matter Mater. Phys.*, 1998, **58**, 11009.

148 J. Zhou, Q. Wang, Q. Sun, X. S. Chen, Y. Kawazoe and P. Jena, Ferromagnetism in semi-hydrogenated graphene sheet, *Nano Lett.*, 2009, **9**, 3867–3870.

149 M. Wu, J. D. Burton, E. Y. Tsybal, X. C. Zheng and P. Jena, Hydroxyl-decorated graphene systems as candidates for organic metal-free ferroelectrics, multiferroics, and high-performance proton battery cathode materials, *Phys. Rev. B: Condens. Matter Mater. Phys.*, 2013, **87**, 081406.

150 J. Li, Y. Liu, Y. Zhang, H. L. Cai and R. G. Xiong, Molecular ferroelectrics: where electronics meet biology, *Phys. Chem. Chem. Phys.*, 2013, **15**, 20786–20796.

151 S. M. Tan, Z. Sofer and M. Pumera, Biomarkers detection on hydrogenated graphene surfaces: towards applications of graphane in biosensing, *Electroanalysis*, 2013, **25**, 703–705.

152 B. Strojny, N. Kurantowicz, E. Sawosz, M. Grodzik, S. Jaworski, M. Kutwin, M. Wierzbicki, A. Hotowy,

L. Lipinska and A. Chwalibog, Long term influence of carbon nanoparticles on health and liver status in rats, *PLoS One*, 2015, **10**(12), e0144821.

153 I. I. Kulakova, Surface chemistry of nanodiamonds, *Phys. Solid State*, 2004, **46**(4), 636e43.

154 N. Kurantowicz, E. Sawosz, S. Jaworski, M. Kutwin, B. Strojny, M. Wierzbicki, J. Szeliga, A. Hotowy, L. Lipinska and R. J. Kozinski, Interaction of graphene family materials with *Listeria monocytogenes* and *Salmonella enterica*, *Nanoscale Res. Lett.*, 2015, **10**(1), 23.

155 M. Wierzbicki, E. Sawosz, M. Grodzik, M. Prasek, S. Jaworski and A. Chwalibog, Comparison of anti-angiogenic properties of pristine carbon nanoparticles, *Nanoscale Res. Lett.*, 2013, **8**(1), 195.

156 M. Maas, Carbon nanomaterials as antibacterial colloids, *Materials*, 2016, **9**(8), 617.

157 H. W. Kroto, J. R. Heath, S. C. O'Brien, R. F. Curl and R. E. Smalley, C60: buckminsterfullerene, *Nature*, 1985, **318**(6042), 162.

158 G. Hong, S. Diao, A. L. Antaris and H. Dai, Carbon nanomaterials for biological imaging and nanomedicinal therapy, *Chem. Rev.*, 2015, **115**(19), 10816–10906.

159 W. Krätschmer, L. D. Lamb, K. Fostiropoulos and D. R. Huffman, Solid C60: a new form of carbon, *Nature*, 1990, **347**(6291), 354.

160 L. T. Scott, M. M. Boorum, B. J. McMahon, S. Hagen, J. Mack, J. Blank, H. Wegner and A. J. S. de Meijere, A rational chemical synthesis of C60, *Science*, 2002, **295**(5559), 1500–1503.

161 C. Cha, S. R. Shin, N. Annabi, M. R. Dokmeci and A. Khademhosseini, Carbon-based nanomaterials: multifunctional materials for biomedical engineering, *ACS Nano*, 2013, **7**(4), 2891–2897.

162 S. Iijima, Helical microtubules of graphitic carbon, *Nature*, 1991, **354**(6348), 56.

163 A. Thess, R. Lee, P. Nikolaev, H. Dai, P. Petit, J. Robert, C. Xu, Y. H. Lee, S. G. Kim, A. G. Rinzler, D. T. Colbert, G. E. Scuseria, D. Tomanek, J. E. Fischer and R. E. Smalley, Crystalline ropes of metallic carbon nanotubes, *Science*, 1996, **273**(5274), 483–487.

164 M. José-Yacamán, M. Miki-Yoshida, L. Rendon and J. J. Santiesteban, Catalytic growth of carbon microtubules with fullerene structure, *Appl. Phys. Lett.*, 1993, **62**(6), 657–659.

165 X. Sun, S. Zaric, D. Daranciang, K. Welsher, Y. Lu, X. Li and H. Dai, Optical properties of ultrashort semiconducting single-walled carbon nanotube capsules down to sub-10 nm, *J. Am. Chem. Soc.*, 2008, **130**(20), 6551–6555.

166 J. T. Robinson, K. Welsher, S. M. Tabakman, S. P. Sherlock, H. Wang, R. Luong and H. Dai, High performance in vivo near-IR (>1 mm) imaging and photothermal cancer therapy with carbon nanotubes, *Nano Res.*, 2010, **3**(11), 779–793.

167 T. Murakami, H. Nakatsuji, M. Inada, Y. Matoba, T. Umeyama, M. Tsujimoto, S. Isoda, M. Hashida and H. Imahori, Photodynamic and photothermal effects of semiconducting and metallic-enriched single-walled carbon nanotubes, *J. Am. Chem. Soc.*, 2012, **134**(43), 17862–17865.

168 S. Iijima, C. Brabec, A. Maiti and J. Bernholc, Structural flexibility of carbon nanotubes, *J. Chem. Phys.*, 1996, **104**(5), 2089–2092.

169 H. Wei, Y. Wei, Y. Wu, L. Liu, S. Fan and K. Jiang, High-strength composite yarns derived from oxygen plasma modified superaligned carbon nanotube arrays, *Nano Res.*, 2013, **6**(3), 208–215.

170 M. A. Correa-Duarte, N. Wagner, J. Rojas-Chapana, C. Morsczeck, M. Thie and M. Giersig, Fabrication and biocompatibility of carbon nanotube-based 3D networks as scaffolds for cell seeding and growth, *Nano Lett.*, 2004, **4**(11), 2233–2236.

171 X. Shi, B. Sitharaman, Q. P. Pham, F. Liang, K. Wu, W. Edward Billups, L. J. Wilson and A. G. Mikos, Fabrication of porous ultra-short singlewalled carbon nanotube nanocomposite scaffolds for bone tissue engineering, *Biomaterials*, 2007, **28**(28), 4078–4090.

172 E. K. Chow, X.-Q. Zhang, M. Chen, R. Lam, E. Robinson, H. Huang, D. Schaffer, E. Osawa, A. Goga and D. J. Ho, Nanodiamond therapeutic delivery agents mediate enhanced chemoresistant tumor treatment, *Sci. Transl. Med.*, 2011, **3**(73), 73ra21.

173 K. Bhattacharya, S. P. Mukherjee, A. Gallud, S. C. Burkert, S. Bistarelli, S. Bellucci, M. Bottini, A. Star and B. Fadell, Biological interactions of carbon-based nanomaterials: from coronation to degradation, *Biol. Med.*, 2016, **12**(2), 333–351.

174 V. N. Mochalin, O. Shenderova, D. Ho and Y. Gogotsi, The properties and applications of nanodiamonds, *Nat. Nanotechnol.*, 2012, **7**(1), 11.

175 V. Y. Dolmatov, Detonation-synthesis nanodiamonds: synthesis, structure, properties and applications, *Russ. Chem. Rev.*, 2007, **76**(4), 339–360.

176 A. Manke, L. Wang and Y. Rojanasakul, Pulmonary toxicity and fibrogenic response of carbon nanotubes, *Toxicol. Mech. Methods*, 2013, **23**(3), 196–206.

177 K. P. Loh, D. Ho, G. N. C. Chiu, D. T. Leong, G. Pastorin and E. K.-H. Chow, Clinical applications of carbon nanomaterials in diagnostics and therapy, *Adv. Mater.*, 2018, **30**(47), 1802368.

178 M. Mohajeri, B. Behnam and A. Sahebkar, Biomedical applications of carbon nanomaterials: drug and gene delivery potentials, *J. Cell Physiol.*, 2019, **234**(1), 298–319.

179 A. Bianco, K. Kostarelos and M. Prato, Opportunities and challenges of carbon-based nanomaterials for cancer therapy, *Expert Opin. Drug Delivery*, 2008, **5**(3), 331–342.

180 C.-H. Choi, ABC transporters as multidrug resistance mechanisms and the development of chemosensitizers for their reversal, *Cancer Cell Int.*, 2005, **5**(1), 30.

181 J. I. Fletcher, M. Haber, M. J. Henderson and M. D. Norris, ABC transporters in cancer: more than just drug efflux pumps, *Nat. Rev. Cancer*, 2010, **10**(2), 147.

182 T.-B. Toh, D.-K. Lee, W. Hou, L. N. Abdullah, J. Nguyen, D. Ho and E. K. Chow, Nanodiamond-mitoxantrone com-

plexes enhance drug retention in chemoresistant breast cancer cells, *Mol. Pharm.*, 2014, **11**(8), 2683–2691.

183 H. B. Man, H. Kim, H.-J. Kim, E. Robinson, W. K. Liu, E. K.-H. Chow and D. Ho, Synthesis of nanodiamond-dau-norubicin conjugates to overcome multidrug chemoresistance in leukemia, *Nanomedicine*, 2014, **10**(2), 359–369.

184 H. Huang, E. Pierstorff, E. Osawa and D. Ho, Active nano-diamond hydrogels for chemotherapeutic delivery, *Nano Lett.*, 2007, **7**(11), 3305e14.

185 X. Wang, X. C. Low, W. Hou, L. N. Abdullah, T. B. Toh, M. Mohd Abdul Rashid, D. Ho and E. K.-H. Chow, Epirubicin-adsorbed nanodiamonds kill chemoresistant hepatic cancer stem cells, *ACS Nano*, 2014, **8**(12), 12151–12166.

186 H. B. Man, H. Kim, H.-J. Kim, E. Robinson, W. K. Liu, E. K.-H. Chow and D. Ho, Synthesis of nanodiamond-dau-norubicin conjugates to overcome multidrug chemoresistance in leukemia, *Nanomedicine*, 2014, **10**(2), 359–369.

187 M. Grodzik, E. Sawosz, M. Wierzbicki, P. Orlowski, A. Hotowy, T. Niemiec, M. Szmidt, K. Mitura and A. J. Chwalibog, Nanoparticles of carbon allotropes inhibit glioblastoma multiforme angiogenesis in ovo, *Int. J. Nanomed.*, 2011, **6**, 3041.

188 A. Montellano, T. Da Ros, A. Bianco and M. Prato, Fullerene C60 as a multifunctional system for drug and gene delivery, *Nanoscale*, 2011, **3**(10), 4035–4041.

189 L. R. Arias and L. Yang, Inactivation of bacterial pathogens by carbon nanotubes in suspensions, *Langmuir*, 2009, **25**(5), 3003–3012.

190 Z. Liu, K. Chen, C. Davis, S. Sherlock, Q. Cao, X. Chen and H. Dai, Drug delivery with carbon nanotubes for in vivo cancer treatment, *Cancer Res.*, 2008, **68**(16), 6652–6660.

191 Z. Liu, A. C. Fan, K. Rakhra, S. Sherlock, A. Goodwin, X. Chen, Q. Yang, D. W. Felsher and H. Dai, Supramolecular stacking of doxorubicin on carbon nanotubes for in vivo cancer therapy, *Angew. Chem., Int. Ed.*, 2009, **121**(41), 7804–7808.

192 C. Palm, M. Jayamanne, M. Kjellander and M. Hällbrink, Peptide degradation is a critical determinant for cell-penetrating peptide uptake, *Biochim. Biophys. Acta*, 2007, **1768**(7), 1769e76.

193 C. Johnson-Léger, C. A. Power, G. Shomade, J. P. Shaw and A. E. Proudfoot, Protein therapeutics - lessons learned and a view of the future, *Expert Opin. Biol. Ther.*, 2006, **6**(1), 1–7.

194 Y. Lu, J. Yang and E. Sega, Issues related to targeted delivery of proteins and peptides, *AAPS J.*, 2006, **8**(3), E466–E478.

195 L.-C. L. Huang and H.-C. Chang, Adsorption and immobilization of cytochromeconnanodiamonds, *Langmuir*, 2004, **20**(14), 5879–5884.

196 M. Gu, X. Wang, T. B. Toh, L. Hooi, D. G. Tenen and E. K. H. Chow, Nanodiamond-based platform for intra-cellular-specific delivery of therapeutic peptides against hepatocellular carcinoma, *Adv. Ther.*, 2018, **1**(8), 1800110.

197 R. A. Shimkunas, E. Robinson, R. Lam, S. Lu, X. Xu, X.-Q. Zhang, H. Huang, E. Osawa and D. Ho, Nanodiamond-insulin complexes as pH dependent protein delivery vehicles, *Biomaterials*, 2009, **30**(29), 5720–5728.

198 Y. Kuo, T.-Y. Hsu, Y.-C. Wu and H.-C. Chang, Fluorescent nanodiamond as a probe for the intercellular transport of proteins in vivo, *Biomaterials*, 2013, **34**(33), 8352e60.

199 X. Wang, M. Gu, T. B. Toh, N. L. B. Abdullah and E. K.-H. Chow, Stimuli responsive nanodiamond-based bio-sensor for enhanced metastatic tumor site detection, *SLAS Technol.*, 2018, **23**(1), 44–56.

200 A. H. Smith, E. M. Robinson, X.-Q. Zhang, E. K. Chow, Y. Lin, E. Osawa, J. Xi and D. Ho, Triggered release of therapeutic antibodies from nanodiamond complexes, *Nanoscale*, 2011, **3**(7), 2844–2848.

201 N. W. Kam and H. Dai, Carbon nanotubes as intracellular protein transporters: generality and biological functionality, *J. Am. Chem. Soc.*, 2005, **127**(16), 6021–6026.

202 H. Yin, R. L. Kanasty, A. A. Eltoukhy, A. J. Vegas, J. R. Dorkin and D. G. Anderson, Non-viral vectors for gene-based therapy, *Nat. Rev. Genet.*, 2014, **15**(8), 541.

203 S. Nayak and R. W. Herzog, Progress and prospects: immune responses to viral vectors, *Gene Ther.*, 2010, **17**(3), 295.

204 M. Ramamoorth and A. Narvekar, Non viral vectors in gene therapy- an overview, *J. Clin. Diagn. Res.*, 2015, **9**(1), GE01–GE06.

205 M. Riley and W. Vermerris, Recent advances in nanomaterials for gene delivery-a review, *Nanomaterials*, 2017, **7**(5), 94.

206 V. Petrakova, V. Benson, M. Buncek, A. Fiserova, M. Ledvina, J. Stursa, P. Cigler and M. Nesladek, Imaging of transfection and intracellular release of intact, non-labeled DNA using fluorescent nanodiamonds, *Nanoscale*, 2016, **8**(23), 12002–12012.

207 X.-Q. Zhang, M. Chen, R. Lam, X. Xu, E. Osawa and D. Ho, Polymerfunctionalizednanodiamond platforms as vehicles for gene delivery, *ACS Nano*, 2009, **3**(9), 2609–2616.

208 M. Chen, X.-Q. Zhang, H. B. Man, R. Lam, E. K. Chow and D. Ho, Nanodiamond vectors functionalized with poly-ethylenimine for siRNA delivery, *J. Phys. Chem. Lett.*, 2010, **1**(21), 3167e71.

209 A. Alhaddad, M.-P. Adam, J. Botsoa, G. Dantelle, S. Perruchas, T. Gacoin, C. Mansuy, S. Lavielle, C. Malvy, F. Treussart and J. R. Bertrand, Nanodiamond as a vector for siRNA delivery to Ewing sarcoma cells, *Small*, 2011, **7**(21), 3087–3095.

210 K. Ushizawa, Y. Sato, T. Mitsumori, T. Machinami, T. Ueda and T. Ando, Covalent immobilization of DNA on diamond and its verification by diffuse reflectance infrared spectroscopy, *Chem. Phys. Lett.*, 2002, **351**(1–2), 105–108.

211 H. Isobe, W. Nakanishi, N. Tomita, S. Jinno, H. Okayama and E. Nakamura, Gene delivery by aminofullerenes: structural requirements for efficient transfection, *Chem. – Asian J.*, 2006, **1**(1–2), 167–175.

212 C. Klumpp, L. Lacerda, O. Chaloin, T. D. Ros, K. Kostarelos, M. Prato and A. Bianco, Multifunctionalised cationic fullerene adducts for gene transfer: design, synthesis and DNA complexation, *Chem. Commun.*, 2007, (36), 3762–3764.

213 S. R. Shin, K. S. Jin, C. K. Lee, S. I. Kim, G. M. Spinks, I. So, J.-H. Jeon, T. M. Kang, J. Y. Mun, S.-S. Han, M. Ree and S. J. Kim, Fullerene attachment enhances performance of a DNA nanomachine, *Adv. Mater.*, 2009, 21(19), 1907–1910.

214 B. Sitharaman, T. Y. Zakharian, A. Saraf, P. Misra, J. Ashcroft, S. Pan, Q. P. Pham, A. G. Mikos, L. J. Wilson and D. A. Engler, Water-soluble fullerene (C60) derivatives as nonviral gene-delivery vectors, *Mol. Pharm.*, 2008, 5(4), 567–578.

215 R. Maeda-Mamiya, E. Noiri, H. Isobe, W. Nakanishi, K. Okamoto, K. Doi, T. Sugaya, T. Izumi, T. Homma and E. Nakamura, In vivo gene delivery by cationic tetraamino fullerene, *Proc. Natl. Acad. Sci. U. S. A.*, 2010, 107(12), 5339–5344.

216 L. Gao, L. Nie, T. Wang, Y. Qin, Z. Guo, D. Yang and X. Yan, Carbon nanotube delivery of the GFP gene into mammalian cells, *ChemBioChem*, 2006, 7(2), 239–242.

217 W. Qin, K. Yang, H. Tang, L. Tan, Q. Xie, M. Ma, Y. Zhang, S. Yao and S. B. Biointerfaces, Improved GFP gene transfection mediated by polyamidoamine dendrimer-functionalized multi-walled carbon nanotubes with high biocompatibility, *Colloids Surf., B*, 2011, 84(1), 206–213.

218 Y. Hao, P. Xu, C. He, X. Yang, M. Huang, J. Xing and J. Chen, Impact of carbodiimide crosslinker used for magnetic carbon nanotube mediated GFP plasmid delivery, *Nanotechnology*, 2011, 22(28), 285103.

219 Y. Inoue, H. Fujimoto, T. Ogino and H. Iwata, Site-specific gene transfer with high efficiency onto a carbon nanotube-loaded electrode, *J. R. Soc., Interface*, 2008, 5(25), 909–918.

220 N. W. S. Kam, Z. Liu and H. Dai, Functionalization of carbon nanotubes via cleavable disulfide bonds for efficient intracellular delivery of siRNA and potent gene silencing, *J. Am. Chem. Soc.*, 2005, 127(36), 12492–12493.

221 X. Wang, J. Ren and X. Qu, Targeted RNA interference of cyclin A2 mediated by functionalized single-walled carbon nanotubes induces proliferation arrest and apoptosis in chronic myelogenous leukemia K562 cells, *ChemMedChem*, 2008, 3(6), 940e5.

222 R. Krajcik, A. Jung, A. Hirsch, W. Neuhuber and O. Zolk, Functionalization of carbon nanotubes enables non-covalent binding and intracellular delivery of small interfering RNA for efficient knockdown of genes, *Biochem. Biophys. Res. Commun.*, 2008, 369(2), 595–602.

223 M. S. Ladeira, V. A. Andrade, E. R. M. Gomes, C. J. Aguiar, E. R. Moraes, J. S. Soares, E. E. Silva, R. G. Lacerda, L. O. Ladeira, A. Jorio, P. Lima, M. Fatima Leite, R. R. Resende and S. Guatimosim, Highly efficient siRNA delivery system into human and murine cells using single-wall carbon nanotubes, *Nanotechnology*, 2010, 21(38), 385101.

224 G. Bartholomeusz, P. Cherukuri, J. Kingston, L. Cognet, R. Lemos, T. K. Leeuw, L. Gumbiner-Russo, R. B. Weisman and G. Powis, In vivo therapeutic silencing of hypoxia-inducible factor 1 alpha (HIF-1a) using single-walled carbon nanotubes noncovalently coated with siRNA, *Nano Res.*, 2009, 2(4), 279–291.

225 J. T. Lanner, J. D. Bruton, Y. Assefaw-Redda, Z. Andronache, S. J. Zhang, D. Severa, Z.-B. Zhang, W. Melzer, S.-L. Zhang, A. Katz and H. Westerblad, Knockdown of TRPC3 with siRNA coupled to carbon nanotubes results in decreased insulin-mediated glucose uptake in adult skeletal muscle cells, *FASEB J.*, 2009, 23(6), 1728–1738.

226 Z. Liu, M. Winters, M. Holodniy and H. Dai, siRNA delivery into human T cells and primary cells with carbon-nanotube transporters, *Angew. Chem., Int. Ed.*, 2007, 119(12), 2069–2073.

227 D. P. O'Neal, L. R. Hirsch, N. J. Halas, J. D. Payne and J. L. West, Photothermal tumor ablation in mice using near infrared-absorbing nanoparticles, *Cancer Lett.*, 2004, 209(2), 171–176.

228 N. W. S. Kam, M. O'Connell, J. A. Wisdom and H. Dai, Carbon nanotubes as multifunctional biological transporters and near-infrared agents for selective cancer cell destruction, *Proc. Natl. Acad. Sci. U. S. A.*, 2005, 102(33), 11600–11605.

229 H. K. Moon, S. H. Lee and H. C. Choi, In vivo near-infrared mediated tumor destruction by photothermal effect of carbon nanotubes, *ACS Nano*, 2009, 3(11), 3707–3713.

230 Y. Yamakoshi, N. Umezawa, A. Ryu, K. Arakane, N. Miyata, Y. Goda, T. Masumizu and T. Nagano, Active oxygen species generated from photoexcited fullerene (C60) as potential medicines: O<sub>2</sub>-versus 1O<sub>2</sub>, *J. Am. Chem. Soc.*, 2003, 125(42), 12803–12809.

231 Y. Iwamoto and Y. Yamakoshi, A highly water-soluble C60-NVP copolymer: a potential material for photodynamic therapy, *Chem. Commun.*, 2006, (46), 4805–4807.

232 Z. Markovic and V. Trajkovic, Biomedical potential of the reactive oxygen species generation and quenching by fullerenes (C60), *Biomaterials*, 2008, 29(26), 3561–3573.

233 S. K. Sharma, L. Y. Chiang and M. R. Hamblin, Photodynamic therapy with fullerenes in vivo: reality or a dream?, *Nanomedicine*, 2011, 6(10), 1813–1825.

234 L. Wang, J. Shi, R. Liu, Y. Liu, J. Zhang, X. Yu, J. Gao, C. Zhang and Z. Zhang, Photodynamic effect of functionalized single-walled carbon nanotubes: a potential sensitizer for photodynamic therapy, *Nanoscale*, 2014, 6(9), 4642–4651.

235 J. Shi, R. Ma, L. Lei Wang, J. Zhang, R. Liu, Y. Liu, X. Yu, J. Gao, L. Li, L. Hou and Z. Zhang, The application of hyaluronic acid derivatized carbon nanotubes in hematoporphyrin monomethyl ether-based photodynamic therapy for in vivo and in vitro cancer treatment, *Int. J. Nanomed.*, 2013, 8, 2361.

236 K. Welsher, S. P. Sherlock and H. Dai, Deep-tissue anatomical imaging of mice using carbon nanotube fluorophores, *Nanoscale*, 2014, 6(9), 4642–4651.

phores in the second nearinfrared window, *Proc. Natl. Acad. Sci. U. S. A.*, 2011, **108**(22), 8943–8948.

237 G. Hong, J. C. Lee, J. T. Robinson, U. Raaz, L. Xie, N. F. Huang, J. P. Cooke and H. Dai, Multifunctional in vivo vascular imaging using near-infrared II fluorescence, *Nat. Med.*, 2012, **18**(12), 1841.

238 G. Hong, S. Diao, J. Chang, A. L. Antaris, C. Chen, B. Zhang, S. Zhao, D. N. Atochin, P. L. Huang, K. I. Andreasson, C. J. Kuo and H. Dai, Throughskull fluorescence imaging of the brain in a new near-infrared window, *Nat. Photonics*, 2014, **8**(9), 723.

239 T.-J. Wu, Y.-K. Tzeng, W.-W. Chang, C.-A. Cheng, Y. Kuo, C.-H. Chien, H.-C. Chang and J. Yu, Tracking the engraftment and regenerative capabilities of transplanted lung stem cells using fluorescent nanodiamonds, *Nat. Nanotechnol.*, 2013, **8**(9), 682.

240 J. Jeong, J. Jung, M. Choi, J. W. Kim, S. J. Chung, S. Lim, H. Lee and B. H. Chung, Color-tunable photoluminescent fullerene nanoparticles, *Adv. Mater.*, 2012, **24**(15), 1999–2003.

241 N. Levi, R. R. Hantgan, M. O. Lively, D. L. Carroll and G. L. Prasad, C 60-Fullerenes: detection of intracellular photoluminescence and lack of cytotoxic effects, *J. Nanobiotechnol.*, 2006, **4**(1), 14.

242 J. Jeong, M. Cho, Y. T. Lim, N. W. Song and B. H. Chung, Synthesis and characterization of a photoluminescent nanoparticle based on fullerene-silica hybridization, *Angew. Chem., Int. Ed.*, 2009, **48**(29), 5296–5299.

243 S. Lin, D. X. Jones, A. S. Mount and P. C. Ke, *Fluorescence of water-soluble fullerenes in biological systems*, NSTI-Nanotech, 2007, pp. 238–241.

244 L. Rondin, G. Dantelle, A. Slablab, F. Grosshans, F. Treussart, P. Bergonzo, S. Perruchas, T. Gacoin, M. Chaigneau and H.-C. Chang, Surface-induced charge state conversion of nitrogen-vacancy defects in nanodiamonds, *Mater. Sci.*, 2010, **82**(11), 115449.

245 M. W. Doherty, N. B. Manson, P. Delaney, F. Jelezko, J. Wrachtrup and L. C. L. Hollenberg, The nitrogen-vacancy colourcentre in diamond, *Phys. Rep.*, 2013, **528**(1), 1–45.

246 V. N. Mochalin, O. Shenderova, D. Ho and Y. Gogotsi, The properties and applications of nanodiamonds, *Nat. Nanotechnol.*, 2012, **7**(1), 11.

247 N. W. Shi Kam, T. C. Jessop, P. A. Wender and H. Dai, Nanotube molecular transporters: internalization of carbon nanotube-protein conjugates into mammalian cells, *J. Am. Chem. Soc.*, 2004, **126**(22), 6850–6851.

248 P. Cherukuri, S. M. Bachilo, S. H. Litovsky and R. B. Weisman, Nearinfrared fluorescence microscopy of single-walled carbon nanotubes in phagocytic cells, *J. Am. Chem. Soc.*, 2004, **126**(48), 15638–15639.

249 Z. Liu, C. Davis, W. Cai, L. He, X. Chen and H. Dai, Circulation and longterm fate of functionalized, biocompatible single-walled carbon nanotubes in mice probed by Raman spectroscopy, *Proc. Natl. Acad. Sci. U. S. A.*, 2008, **105**(5), 1410–1415.

250 C. Wang, X. Ma, S. Ye, L. Cheng, K. Yang, L. Guo, C. Li, Y. Li and Z. Liu, Protamine functionalized single-walled carbon nanotubes for stem cell labeling and in vivo Raman/Magnetic resonance/photoacoustic triple-modal imaging, *Adv. Funct. Mater.*, 2012, **22**(11), 2363–2375.

251 S. Keren, C. Zavaleta, Z. Cheng, A. de La Zerda, O. Gheysens and S. S. Gambhir, Noninvasive molecular imaging of small living subjects using Raman spectroscopy, *Proc. Natl. Acad. Sci. U. S. A.*, 2008, **105**(15), 5844–5849.

252 C. Zavaleta, A. De La Zerda, Z. Liu, S. Keren, Z. Cheng, M. Schipper, X. Chen, H. Dai and S. S. Gambhir, Noninvasive Raman spectroscopy in living mice for evaluation of tumor targeting with carbon nanotubes, *Nano Lett.*, 2008, **8**(9), 2800–2805.

253 A. De La Zerda, C. Zavaleta, S. Keren, S. Vaithilingam, S. Bodapati, Z. Liu, J. Levi, B. R. Smith, T.-J. Ma, O. Oralkan, Z. Cheng, X. Chen, H. Dai, B. T. Khuri-Yakub and S. S. Gambhir, Carbon nanotubes as photoacoustic molecular imaging agents in living mice, *Nat. Nanotechnol.*, 2008, **3**(9), 557.

254 E. I. Galanzha, E. V. Shashkov, T. Kelly, J.-W. Kim, L. Yang and V. P. Zharov, In vivo magnetic enrichment and multiplex photoacoustic detection of circulating tumour cells, *Nat. Nanotechnol.*, 2009, **4**(12), 855.

255 M. B. A. F. Martins, M. L. Corvo, P. Marcelino, H. S. Marinho, G. Feio and A. Carvalho, New long circulating magnetoliposomes as contrast agents for detection of ischemia-reperfusion injuries by MRI, *Nanomedicine*, 2014, **10**(1), 207–214.

256 P. Caravan, J. J. Ellison, T. J. McMurry and R. B. Lauffer, Gadolinium(III) chelates as MRI contrast agents: structure, dynamics, and applications, *Chem. Rev.*, 1999, **99**(9), 2293–2352.

257 M. Perazella, Gadolinium-contrast toxicity in patients with kidney disease: nephrotoxicity and nephrogenic systemic fibrosis, *Curr. Drug Saf.*, 2008, **3**(1), 67–75.

258 M. A. Perazella, Current status of gadolinium toxicity in patients with kidney disease, *Clin. J. Am. Soc. Nephrol.*, 2009, **4**(2), 461–469.

259 W. Hou, T. B. Toh, L. N. Abdullah, T. W. Z. Yvonne, K. J. Lee, I. Guenther and E. K.-H. Chow, Nanodiamond-manganese dual mode MRI contrast agents for enhanced liver tumor detection, *J. Nanomed. Nanotechnol.*, 2017, **13**(3), 783–793.

260 Z. Chen, L. Ma, Y. Liu and C. Chen, Applications of functionalized fullerenes in tumor theranostics, *Theranostics*, 2012, **2**(3), 238.

261 H. Kato, Y. Kanazawa, M. Okumura, A. Taninaka, T. Yokawa and H. Shinohara, Lanthanoid endohedral metallofullerenols for MRI contrast agents, *J. Am. Chem. Soc.*, 2003, **125**(14), 4391–4397.

262 K. B. Ghiassi, M. M. Olmstead and A. L. Balch, Gadolinium-containing endohedral fullerenes: structures and function as magnetic resonance imaging (MRI) agents, *Dalton Trans.*, 2014, **43**(20), 7346–7358.

263 C. Richard, B.-T. Doan, J.-C. Beloeil, M. Bessodes, É. Tóth and D. Scherman, Noncovalent functionalization of carbon nanotubes with amphiphilic Gd<sup>3+</sup> chelates: toward powerful T1 and T2 MRI contrast agents, *Nano Lett.*, 2008, **8**(1), 232–236.

264 J. H. Choi, F. T. Nguyen, P. W. Barone, D. A. Heller, A. E. Moll, D. Patel, S. A. Boppart and M. S. Strano, Multimodal biomedical imaging with asymmetric single-walled carbon nanotube/iron oxide nanoparticle complexes, *Nano Lett.*, 2007, **7**(4), 861–867.

265 H. Liu, L. Zhang, M. Yan and J. Yu, Carbon nanostructures in biology and medicine, *J. Mater. Chem. B*, 2017, **5**(32), 6437–6450.

266 S. Marchesan, M. Melchionna and M. Prato, Carbon nanostructures for nanomedicine: opportunities and challenges, *Fullerenes, Nanotubes, Carbon Nanostruct.*, 2014, **22**(1–3), 190–195.

267 A. H. Pourasl, M. Ahmadi, M. Rahmani, H. Chin, C. Lim, R. Ismail and M. L. Tan, Analytical modeling of glucose biosensors based on carbon nanotubes, *Nanoscale Res. Lett.*, 2014, **9**(1), 33.

268 X. Tang, S. Bansaruntip, N. Nakayama, E. Yenilmez, Y.-l. Chang and Q. Wang, Carbon nanotube DNA sensor and sensing mechanism, *Nano Lett.*, 2006, **6**(8), 1632–1636.

269 B. Zhao, H. Hu, S. K. Mandal and R. C. Haddon, A bone mimic based on the self-assembly of hydroxyapatite on chemically functionalized single-walled carbon nanotubes, *Chem. Mater.*, 2005, **17**(12), 3235–3241.

270 G.-Z. Jin, M. Kim, U. S. Shin and H.-W. Kim, Neurite outgrowth of dorsal root ganglia neurons is enhanced on aligned nanofibrous biopolymer scaffold with carbon nanotube coating, *Neurosci. Lett.*, 2011, **501**(1), 10–14.

271 S. R. Shin, S. M. Jung, M. Zalabany, K. Kim, P. Zorlutuna, S. Kim, M. Nikkhah, M. Khabiry, M. Azize, J. Kong, K.-t. Wan, T. Palacios, M. R. Dokmeci, H. Bae, X. Tang and A. Khademhosseini, Carbonnanotube- embedded hydrogel sheets for engineering cardiac constructs and bioactuators, *ACS Nano*, 2013, **7**(3), 2369–2380.

272 Y. Wei, X. Mo, P. Zhang, Y. Li, J. Liao, Y. Li, J. Zhang, C. Ning, S. Wang, X. Deng and L. Jiang, Directing stem cell differentiation via electrochemical reversible switching between nanotubes and nanotips of polypyrrolearray, *ACS Nano*, 2017, **11**(6), 5915–5924.

273 S. Pacelli, R. Maloney, A. R. Chakravarti, J. Whitlow, S. Basu, S. Modaresi, S. Gehrke and A. Paul, Controlling adult stem cell behavior using nanodiamond-reinforced hydrogel: implication in bone regeneration therapy, *Sci. Rep.*, 2017, **7**(1), 6577.

274 J. Whitlow, S. Pacelli and A. Paul, Multifunctional nanodiamonds in regenerative medicine: recent advances and future directions, *J. Controlled Release*, 2017, **261**, 62–86.

275 D.-K. Lee, T. Kee, Z. Liang, D. Hsiou, D. Miya, B. Wu, E. Osawa, E. K.-H. Chow, E. C. Sung and M. K. Kang, Clinical validation of a nanodiamond-embedded thermoplastic biomaterial, *Proc. Natl. Acad. Sci. U. S. A.*, 2017, 201711924.

276 D.-K. Lee, S. V. Kim, A. N. Limansubroto, A. Yen, A. Soundia, C. Y. Wang, W. Shi, C. Hong, S. Tetradiis, Y. Kim, N.-H. Park, M. K. Kang and D. Ho, Nanodiamond-gutta percha composite biomaterials for root canal therapy, *ACS Nano*, 2015, **9**(11), 11490–11501.

277 C. M. Friedman, J. L. Sandrik, M. A. Heuer and G. W. Rapp, Composition and mechanical properties of gutta-percha endodontic points, *J. Dent. Res.*, 1975, **54**(5), 921–925.

278 X. Chang, M. Zeng, K. Liu and L. Fu, *Adv. Mater.*, 2020, **32**, 1907226.

279 H. Fang, J. Yang, M. Wen and Q. Wu, *Adv. Mater.*, 2018, **30**, 1705698.

280 S. E. Skrabalak, *Science*, 2018, **359**, 1467.

281 Y. Yao, Z. Liu, P. Xie, Z. Huang, T. Li, D. Morris, Z. Finfrock, J. Zhou, M. Jiao, J. Gao, Y. Mao, J. Miao, P. Zhang, R. Shahbazian-Yassar, C. Wang, G. Wang and L. Hu, *Sci. Adv.*, 2020, **6**, eaaz0510.

282 T. Löffler, A. Savan, H. Meyer, M. Meischein, V. Strotkötter, A. Ludwig and W. Schuhmann, *Angew. Chem., Int. Ed.*, 2020, **59**, 5844–5850.

283 W. Zhang, P. K. Liaw and Y. Zhang, *Sci. China Mater.*, 2018, **61**, 2–22.

284 H.-J. Qiu, G. Fang, Y. Wen, P. Liu, G. Xie, X. Liu and S. Sun, *J. Mater. Chem. A*, 2019, **7**, 6499–6506.

285 S. Li, X. Tang, H. Jia, H. Li, G. Xie, X. Liu, X. Lin and H.-J. Qiu, *J. Catal.*, 2020, **383**, 164–171.

286 J.-W. Yeh, S.-K. Chen, S.-J. Lin, J.-Y. Gan, T.-S. Chin, T.-T. Shun, C.-H. Tsau and S.-Y. Chang, *Adv. Eng. Mater.*, 2004, **6**, 299–303.

287 Z. Jin, J. Lv, H. Jia, W. Liu, H. Li, Z. Chen, X. Lin, G. Xie, X. Liu, S. Sun and H.-J. Qiu, *Small*, 2019, **15**, 1904180.

288 Y. Yao, Z. Huang, P. Xie, S. D. Lacey, R. J. Jacob, H. Xie, F. Chen, A. Nie, T. Pu, M. Rehwoldt, D. Yu, M. R. Zachariah, C. Wang, R. Shahbazian-Yassar, J. Li and L. Hu, *Science*, 2018, **359**, 1489–1494.

289 S. G. Kwon, G. Krylova, P. J. Phillips, R. F. Klie, S. Chattopadhyay, T. Shibata, E. E. Bunel, Y. Liu, V. B. Prakapenka, B. Lee and E. V. Shevchenko, *Nat. Mater.*, 2015, **14**, 215–223.

290 M. Bondesgaard, N. L. N. Broge, A. Mamakhel, M. Bremholm and B. B. Iversen, *Adv. Funct. Mater.*, 2019, **29**, 1905933.

291 M. Vara, L. T. Roling, X. Wang, A. O. Elnabawy, Z. D. Hood, M. Chi, M. Mavrikakis and Y. Xia, *ACS Nano*, 2017, **11**, 4571–4581.

292 C. S. Bonifacio, S. Carenco, C. H. Wu, S. D. House, H. Bluhm and J. C. Yang, *Chem. Mater.*, 2015, **27**, 6960–6968.

293 Y. Chen, X. Zhan, S. L. A. Bueno, I. H. Shafei, H. M. Ashberry, K. Chatterjee, L. Xu, Y. Tang and S. E. Skrabalak, *Nanoscale Horiz.*, 2021, **6**, 231.

294 M. Hulander, J. Hong, M. Andersson and F. Gerven, *ACS appl. Mater. Interfaces*, 2009, **1**(5), 1053–1062.

295 R. R. Arvizo, S. Bhattacharya, R. A. Kudgus, K. Giri, R. Bhattacharya and P. Mukherjee, *Chem. Soc. Rev.*, 2012, **41**(7), 2943–2970.

296 S. W. Kim, K. S. Kim, K. Lamsal, Y.-J. Kim, S. B. Kim, M. Jung, S.-J. Sim, H.-S. Kim, S.-J. Chang, J. K. Kim and Y. S. Lee, *J. Microbiol. Biotechnol.*, 2009, **19**(8), 760–764.

297 A. Servin and J. C. White, *Nanoimpact*, 2016, **1**, 9–12.

298 S. T. Thul, B. K. Sarangi and R. A. Pandey, *Expert Opin. Environ. Biol.*, 2013, **2**(1), 1–7.

299 A. C. Barrios, I. A. Medina-Velo, N. Zuverza-Mena, O. E. Dominguez, J. R. Peralta-Videa and J. L. Gardea-Torresdey, *Plant Physiol. Biochem.*, 2017, **110**, 100–107.

300 V. Armendariz, I. Herrera, J. R. Peralta-videa, M. Joseyacaman, H. Troiani, P. Santiago and J. L. Gardea-Torresdey, *J. Nanopart. Res.*, 2004, **6**(4), 377–382.

301 G. Zhu, S. Zhang, E. Song, J. Zheng, R. Hu, X. Fang and W. Tan, *Angew. Chem., Int. Ed.*, 2013, **52**, 5490–5496.